THE MEASUREMENT OF MEMBRANE POTENTIAL IN THE FROG TOE MUSCLE AND SARTORIOUS FIBRES

by

S.I. Ahmad

A thesis submitted to the Faculty of Science
in partial fulfilment of the requirements for the degree of
Master of Science.

Department of Electrical Engineering,
Faculty of Pure and Applied Science,
The University of Ottawa,
Ottawa, Canada.

1964.

ABSTRACT

The membrane potentials in the frog toe and sartorious fibres were investigated by two methods:

In the first method microelectrodes were used and for this method a preamplifier was designed and built having a frequency response dc to 80 kc/s; input current 10^{-10} ampere and input impedance more than 700 megohms.

The resistance of microelectrodes was investigated for a comparison between the values derived theoretically with those measured experimentally. A good agreement was found between theoretical and experimental values for probes having 1-3 megohms resistance. The probes of higher resistance whose dimensions could not be found accurately did not show such a good agreement.

A "Sucrose Gap Method" was used as the second approach. The resting potential measured by this method was 73 mV without compensation and 85 mV with compensation.

ACKNOWLEDGEMENTS

I wish to express my thanks to Dr. G.W. Mainwood for suggesting the problem and for his guidance throughout the course of the research; to Prof. O. Celinski for his help and encouragement in preparation of the thesis; to Mr. R.S. Richards for his help in writing the chapter on pre-amplifier.

This research was made possible through financial support from the National Research Council grant No.-A-871; the Medical Research Council grant No. MA-625 and the Colombo Plan Assistantship Program.

TABLE OF CONTENTS

CHAPTER I

1.1 Introduction - Historical Review of Literature

Galvani, in his classical experiment on "contraction without metals" published in 1794, showed that when the nerve of a muscle was placed between the cut end and the intact surface of a second muscle, the first muscle was stimulated. This phenomenon, although not understood at that time, showed the existence of electromotive force between the cut end and the intact surface of a muscle.

We have been aware of "animal electricity" for over 150 years but its significance in the living animal was debated and the exact mechanism by which currents were generated gave rise to many theories and speculations. Our knowledge of the subject has always been limited by the ability of investigators to measure the small voltages and currents involved in resting and active tissues. Although many ingenious and sensitive recording devices have been made, it is only in the last 10 - 20 years that instruments capable of measuring intracellular electrical events with any accuracy have been devised. Before considering the new instrumentation and methods, the early work and ideas in this field will be briefly reviewed.

The first serious work in the field of animal electricity started with the discoveries of DuBois Reymond (1857) and Bernstein (1869).

The theory presented by DuBois Reymond known as the

"Molecular Theory" can be summed up as follows:

(i) A muscle (or nerve) fibre contains electromotive particles suspended in an indifferent (inactive) material, of which the negative surfaces look towards the end surface of the fibre, the positive surface towards its lateral surface.

(ii) At the natural end surface of muscle, particles of a peculiar kind exist in greater or less degree of development, of which the surface directed to the end of the fibre are positive. The development of these particles is favoured by cold - this constitutes the parelectronomic layer.

(iii) In consequence of excitation the electromotive forces of particles (called by DuBois "molecules") either diminish or assume a different arrangement by virtue of which their external action is impaired. The molecules of parelectronomic layer take no part in this excitatory change.

Bernstein regards the chemical process associated with electrical behavior of tissues as consisting of three stages:

(i) The transition of oxygen from intramolecular to the free state.

(ii) Oxidation.

(iii) Assimilation of oxygen and reconstitution of inogenitic molecule.

He considers the sudden appearance of difference of potential between the excited and unexcited parts - the initial culmination of electrical change - as sign of first stage in the chemical process viz. splitting off of oxygen; the transformation of chemical into mechanical energy having its electrical encomitant

the rapid diminution of difference of potential which occupies the remainder of the period during which the monophasic variation lasts.

These studies prompted the need for developing instruments to record electrical behavior of living tissues. Prof. Hermann devised a special apparatus - the "Fall Rheotome" to give experimental evidence of his theory that the electromotive forces are not pre-existent and that there is a measurable delay between the injury and its effect, i.e. that a certain time is required for these forces to develop proving thereby that the forces in question were not pre-existing forces, which required only unmasking, but that they were called into existence in consequence of changes in the muscular substance produced at the moment of injury. The principle of "Fall Rheotome" was that a galvanometric circuit comprising the muscle was closed at the same moment that the muscle itself was injured and opened at a very short time afterwards. A survey of Prof. Hermann's work appears in the first publication of The Journal of Physiology (1).

In 1886 Prof. Hermann set forth the theory of Capillary Electrometer (2) according to which the rate of polarization of the meniscus of a mercury column when acted upon by a current is proportional to the current strength. Based upon this principle, Capillary Electrometers were designed by Hermann (3) and others (4, 5) and were used successfully for investigation of current strengths of short duration in living tissues (6).

Introduction of vacuum triode amplifiers made it possible to greatly increase the sensitivity of measuring instruments. Forbes in 1920 (7) and Gasser and Newcomer in 1921 (8) used a vacuum tube amplifier with string galvanometer to measure bioelectric currents.

As pointed out by Adrian (9), inertia of the moving system in string galvanometer was an inherent limitation which could not be cured by the use of an amplifier. Adrian in 1926 used vacuum tube amplifier with capillary electrometer in which the inertia factor was extremely small. With the three tube amplifier giving a gain of 1850, the overall sensitivity achieved by him was .01 mv at the input.

In these early studies as described above, and others, the resting and action potentials of nerves and muscles were usually measured between a "killed end" and the region investigated. These potentials would be the actual potential difference across the membranes if there were no external current flow and if the membrane potential at the "killed end" had been reduced to zero, but such conditions were difficult to obtain experimentally. The potential drop developed by current flow in the transition region between the active and the inactive portions reduced the measured resting potential below the membrane resting potential. Moreover the short circuiting in the neighbourhood of active electrode reduced the measured action potential similarly (10).

The introduction of the squid giant axon in 1936 by Young (11) made it possible to considerably reduce the errors in the "killed end" technique of measurement. By working with well cleaned fibres surrounded by as little sea water as possible Cole and Hodgkin in 1939 (12) and Webb and Young in 1940 (13) obtained action potentials of over 70 mv and Steinback in 1940 recorded the resting or injury potential as high as 65 mv (14).

The difficulties with killed end technique were avoided by inserting a very thin Ag-AgCl wire electrode in the fibre to make

direct contact with the protoplasm (Hodgkin and Huxley '39) (15).

In 1940 Curtis and Cole used a micropipette filled with KCl solution as an electrode (16). The action potentials recorded with these microelectrodes were about 90 mv. These studies were done on giant axons which had fibres up to a millimeter in diameter and in which the microelectrodes could be inserted longitudinally.

Independent of the above work, in 1940 Graham, Carlson and Gerard started studies on the muscle fibres (frog sartorii) which were only 70 μ in diameter. The microelectrodes used by these workers were much smaller in diameter for transverse insertion into the fibre. Their work was first reported in 1942 (17, 18). The microelectrodes first used by Graham and Gerard were 5 μ or less outer tip diameter and were filled with isotonic KCl solution. The muscle fibres used were frog sartorii and the average value of measured resting potential was 61.8 mv (19). As discussed by them later they had used microelectrodes which were large (2-5 μ in dia.) and hence caused considerable injury at the fibre membrane. They attributed to this fact the large variation of membrane potentials varying from 40 to 80 mv. Ling and Gerard used electrodes of much smaller diameter ($\ll 1\,\mu$) and recorded an average value of the resting potential as 78.4 mv with $\pm$ 5 mv variation (20).

The microelectrodes with tip diameter much less than one micron, have very high electrical resistance when filled with isotonic KCl solution (100 - 150 MΩ) and cannot be used efficiently

for recording action potentials. Nastuk and Hodgkin (1950) filled these electrodes with 3M KCl solution thus reducing the electrical resistance (to 10-20 MΩ) (21). The ability of potassium to depolarize the membrane is well known. To obtain accurate results it is essential that measurements are not altered by junction potentials (22, 23). This requires careful study of microelectrodes to fix a criterion before they are used for bioelectrical measurements (24).

The microelectrodes used have resistances in the order of tens of megohms. This high resistance combined with electrode's total capacity to ground gives a large time constant. This makes the measuring system unable to record rapid bioelectrical activity unless steps have been taken to reduce the electrical inertia of the instrument. There are several other conditions imposed on the biological amplifiers and these will be discussed in the appropriate sections. We will introduce there the latest of such instruments which has been developed after successive improvements of about thirty years since 1933 when the need for biological amplifiers (special purpose) was first pointed out (25).

1.2 Biological Generator

Biological membrane separates the protoplasm of a living cell from its external environments. The membrane shows specific characteristics of permeability to different organic and inorganic ions. Bernstein (26), Brunings (27) and Lillie (28) from their studies on the biological membranes put forward a theory which

was later developed by Lillie (29) on the basis of a close analogy. According to this theory the surface membrane of a resting nerve fibre is impermeable to certain anions which are present in greater concentration inside the fibre than outside of it. The cations are free to pass through the membrane, but electrostatic attraction of anions will force the cations to remain close to the membrane so that an electrical double layer of ions will be formed. Any stimulation must produce a certain change in ionic concentration at the membrane.

Boyle and Conway (30) found that the membrane of the muscle fibre in the excised sartorious of the frog when maintained under suitable conditions is permeable to potassium and to cations of the same or smaller diameter but impermeable to sodium or larger cations. It is at the same time permeable to the smaller anions such as chloride, bicarbonate, etc., but not to larger anions of the type of phosphocreatine, adenyl pyro phosphoric acid, etc.

Due to difference in concentration of ions in protoplasm and the plasma of a living cell there is a potential difference developed across the membrane separating them. For the case where a non diffusible ion is present on one side Donnan predicted that the value of this potential difference can be found from an equation first proposed by Nernst in 1889 for a concentration cell (Appendix 1).

$$\text{i.e.,} \quad V_A = \frac{RT}{ZF} \ln \frac{[A]_o}{[A]_i} \qquad (1)$$

where

V_A = potential difference corresponding to difference in concentration of diffusible ions A

R = Gas constant (8.31 j/(gm-mole)^{o}K)

F = Faraday constant (96,500 int. coulombs)

Z is the valency of ions : +1 for Na^{+}, K^{+} and -1 for Cl^{-}

$[A]_o$ is the concentration of ions of substance 'A' in outer medium (plasma) (millimol./Kg. of water)

$[A]_i$ is the concentration of ions of substance 'A' in internal medium (protoplasm) (millimol./Kg. of water)

As it would appear from equation 1, we can calculate the potential difference across the membrane if concentrations of diffusible ions are known. Considering for the moment that the potential differences existing due to several such ions are independent of each other we can represent the equivalent circuit of a biological generator as shown in Figure 1.1.

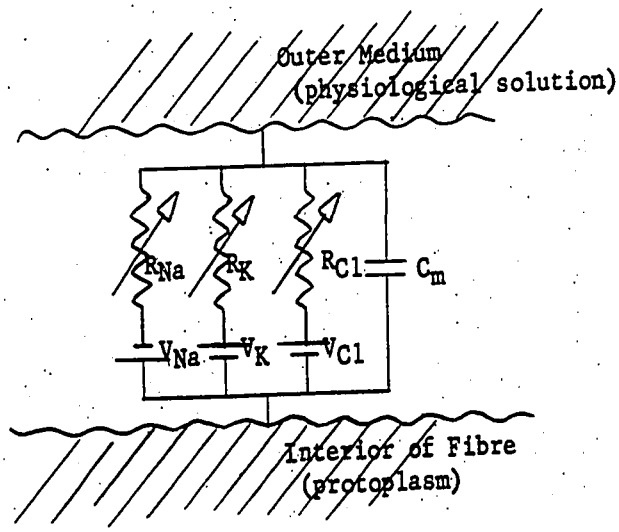

Fig. 1.1 This equivalent circuit is based upon Hodgkin-Huxley (31,32) equations for ionic transport across the membrane. V_{Na}, V_K, V_{Cl} are potentials corresponding to differences in concentration of ions Na^+, K^+ and Cl^-. The polarity of equivalent emfs is determined by the direction of concentration and valency signs of ions e.g. V_{Na} has the polarity as shown because $[Na]_o > [Na]_i$ and Z = +1 for sodium ions.

Table 1.1 gives the values of the concentration as measured by different workers and the calculated values of potentials corresponding to these data.

1.3 Resting Potential

The membrane resting potential is defined as the potential difference between the interior of the fibre and the outer surface of membrane when the fibre is in its normal resting state.

It is now known that the membrane in its normal state is permeable to potassium and chloride ions and almost impermeable to sodium ions (*). Boyle and Conway (30) showed that under these conditions

---

(*) potassium conductance = 0.24 millimho/cm^2; sodium conductance = .0033 millimho/cm^2 (33)

TABLE 1.1 Ionic concentrations and potentials †

No.	Preparation	Potassium concentration (m.mol./kg.H2O) Inside K^+_i	Outside* K^+_o	V_K** mv	Sodium concentration (m.mol./kg.H2O) Inside Na^+_i	Outside Na^+_o	V_{Na} mv	Chloride concentration (m.mol./kg.H2O) Inside Cl^-_i	Outside Cl_o	V_{Cl} mv
1.	Frog sartorious muscle	125	2.5	-104.5	15	120	47.8	1.2	120	-123
2.	Rat cardiac muscle	140	2.7	-105.5	13	150	65.5	-	140	-
3.	Dog skeletal muscle	140	2.7	-105.5	12	150	67.5	-	140	-
4.	Frog nerve	170	2.5	-112.8	37	120	31.8	-	120	-
5.	Carcinus nerve	380	10	- 97.2	-	460	-	-	540	-
6.	Sepia axon	360	10	- 95.6	43	460	63.3	-	540	-
7.	Loligo axon	410	10	- 99.3	49	460	59.8	40	540	-69.5

† Based upon data from Hodgkin, A.L. "The Ionic Basis of Electrical Activity in Nerve and Muscle" Biological Reviews, Cambridge Physiological Society (1951) Vol. 26, pp. 339-401.

* Outside concentrations correspond to ionic concentration in Ringer's solution.

** In equation $V_A = \frac{RT}{Z_A F} \ln \frac{[A]_o}{[A]_i}$

$= \frac{61.5}{Z_A} \log \frac{[A]_o}{[A]_i}$

$\because \ln x = \frac{1}{2.3} \log_{10} x$

R = 8.31 j/(gm-mole)^oK

T = Human body temp. = 37 °C = 310 ^oK

F = Faraday constant 96,500 international coulombs

The entries omitted are for those values which are not significant.

electrolytic balance in muscle relates to true equillibria and the potential difference across the membrane is of the Donnan and not of the diffusion (or concentration type). Accordingly they derived the following expression for the membrane potential:

$$V = \frac{RT}{F} \ln \frac{[C]}{2[K^+]_o} \qquad (2)$$

where C is the total external concentration of diffusible and indiffusible cations as well as anions and uncharged molecules

R, T, F and K^+_i are same as defined previously for equation (1)

Boyle and Conway showed that this relation applies very satisfactorily to a wide range of external potassium concentration in the frog sartorious fibres.

The membrane permeability to K^+, $N\bar{a}$, $C\bar{l}$ and other ions changes with the changes in external concentration of ions, temperature and the state of membrane. These changes are associated with movements of charged particles across the membrane. Using this concept Goldman (34) derived an expression for the potential difference across the membrane. This expression, as modified by Hodgkin and Katz (35), is given below:

$$V = \frac{RT}{F} \ln \frac{P_K [K^+]_o + P_{Na} [N\bar{a}^+]_o + P_{Cl} [C\bar{l}]_i}{P_K [K^+]_i + P_{Na} [Na]_i + P_{Cl} [C\bar{l}]_o}$$

where P_K, P_{Na}, P_{Cl} are the respective coefficients of permeability for the transport of K^+, $N\bar{a}^+$, $C\bar{l}$ ions across the membrane.

The relative values of these coefficients for the membrane of the giant axon of Loligo were found (36) to be as follows:

$$P_K : P_{Na} : P_{Cl} = 1.0 : 0.04 : 0.45$$

Table 1.2 shows calculated value of resting potentials based upon these figures.

TABLE 1.2 Resting potential (V) calculated from

$$V = \frac{RT}{F} \ln \frac{P_K [K]_o + P_{Ka} [Na]_o + P_{Cl} [Cl]_i}{P_K [K]_i + P_{Na} [Na]_i + P_{Cl} [Cl]_o}$$

values of concentrations have been taken from Table 1.1

1.	Frog sartorious muscle	-83.6 mv
2.	Rat cardiac muscle	-84.1 "
3.	Dog skeletal muscle	-84.1 "
4.	Frog nerve	-91.6 "
5.	Carcinus nerve	-82.5 "
6.	Sepia axon	-82.6 "
7.	Logia axon	-70.6 "

It is difficult to quote corresponding values of measured resting potential for these fibres, because these values differ greatly depending upon the measuring technique and the accuracy of the instruments. However in most cases the resting potential has a value between -70 to -90 mv. As an example (Adrian (37) measured the value of resting potential in frog sartorious fibres as -89.2 mv.

1.4 Action Potential

It is well known that cell membrane is capable of showing high degree of selectivity towards Na^+ or K^+ ions depending on the environmental conditions.

Under the resting conditions the membrane may be a 100-times more permeable to K^+ than to Na^+ ions. An excitation of membrane has the following effects in the sequence in which they happen:

(1) Permeability to Na^+ ions increases.

(2) At the peak of Na^+ ions permeability the membrane starts showing an increased permeability to K^+. Because of this the permeability to Na^+ declines.

(3) The fibre cannot be excited until the K^+ permeability also declines and the membrane returns to its original state.

(4) Permeability to Na^+ and K^+ ions reaches a maximum of 42.9 millimho/cm^2 and 24.31 millimho/cm^2 respectively (38).

(5) The movement of Cl^- ions can be regarded as being not very significant.

The wave shape of the potential across the membrane associated with the above changes, known as action potential, is shown in Figure 1.2.

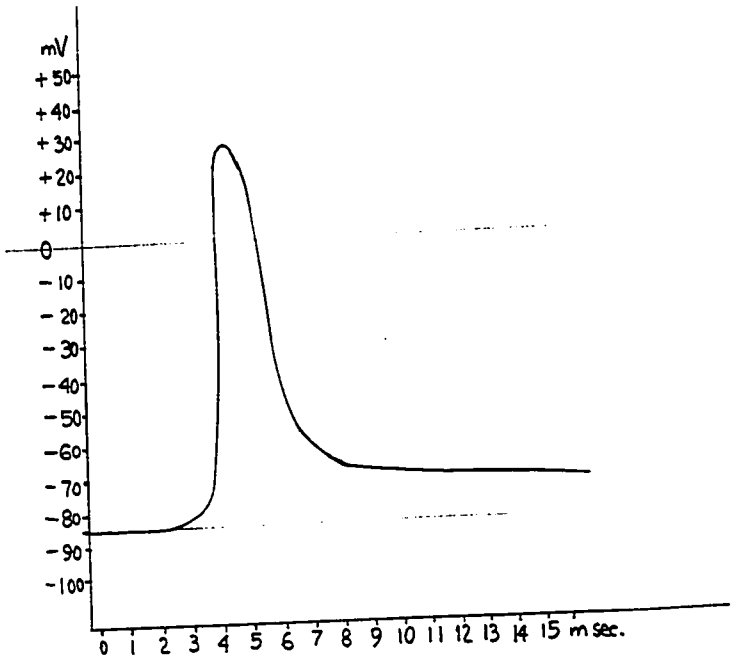

Fig. 1.2 Typical action potential in normal Ringer's fluid (Nastuk & Hodgkin, J. Cell. & Comp. Physiol., Vol. 35, p. 67).

CHAPTER 2

2.1 Muscle Fibre Regarded as an Electric Cable

The muscle fibre consists of a central core of high conductivity (protoplasm) surrounded by an insulating sheath (membrane). (See Fig. 2.1)

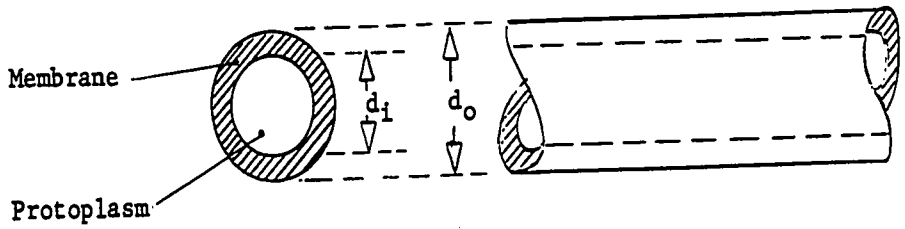

Fig. 2.1

As long as the muscle is not activated the dielectric properties of the membrane remain unchanged and the muscle fibre may be assumed to behave like an electric cable. Therefore we can, by use of the known theory, derive expressions for the membrane capacitance and resistance, and the formulas for these are as given below. (Appendix 2).

$$r_m = \rho_{m.t} \quad \Omega.cm^2 \qquad (2.1)$$

$$C_m = \frac{\varepsilon_m}{36\pi t} .10^{-5} \quad \mu F/cm^2 \qquad (2.2)$$

where r_m is the transverse resistance of membrane per cm. length of fibre ($ohm.cm^2$)

C_m is the membrane capacity per unit length of fibre ($microfarad/cm^2$)

t is the thickness of fibre membrane

ρ_m is the specific resistance of membrane material

ε_m is the relative dielectric constant of membrane material

2.2 Dielectric Properties of Membrane

The cell membrane is chiefly composed of proteins and lipids. Since the experimental evidence indicates that there are about a 100 molecules of lipids for every protein molecule (38), it seems therefore logical to assume that insulating properties of membranes would be akin to those of lipids. In its non-active state the membrane is like an insulating sheath around the protoplasm. The specific resistance of insulating materials depends on their purity (39). The membrane gets its dielectric character from lipids and lipids are oily substances. The proteins present in the membrane form polar structure with lipids (40). This specific structure results in decreased specific resistance and at the same time, in an increase of dielectric constant. In Table 2.1 are given values of specific resistance of some organic structure substances (40).

TABLE 2.1

Item No.	Name of Substance	sp. resistance (ohm.cm)
1	Methyl alcohol	10^5
2	Olive oil (dry)	10^{12}
3	Olive oil (wet with salt solutions)	10^{10}
4	Paraffin	10^{16}
5	Guaiacol (wet with conductivity water)	2.5×10^7

If, in the light of our preceding discussion, we choose the value for specific resistance of membrane as given in Item No. 3 i.e. $\rho_m = 10^{10}\ \Omega.cm$, we find that the corresponding value of the dielectric constant is $\varepsilon_m = 4$. The membrane thickness as measured for

various cells varies between 50-70 $\mathring{A}$ (41).

Substituting these values in equations 2.1 and 2.2, we get

$$r_m = 10^{10} \times 60 \times 10^{-8} \quad \text{ohm.cm}^2$$

$$= 6 \text{ kilo.ohm.cm}^2$$

and

$$C_m = \frac{4}{36\pi \times 60 \times 10^{-8}} \times 10^{-5} \text{ microfarad/cm}^2$$

$$= 0.67 \quad \text{microfarad/cm}^2$$

The measured values of membrane resistance and capacitance are

$$r_m = 1 - 10 \quad \text{kilo.ohm.cm}^2$$
$$C_m = 1 - 10 \quad \text{microfarad/cm}^2 \qquad (42)$$

2.3 Equivalent circuits

A muscle fibre from an electrical point of view is, strictly speaking, a distributed parameter system. By using reasoning similar to that used in transmission line considerations, we can draw the equivalent circuit of a fibre as shown in Fig. 2.2.

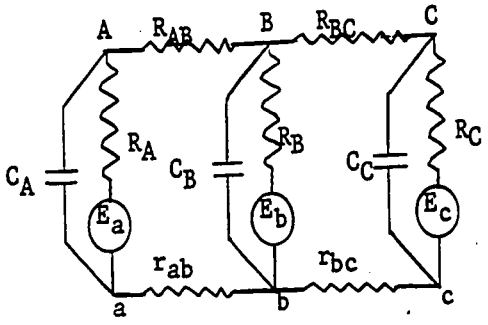

Fig.2.2

R represents resistance of the membrane per unit length and r represents the corresponding protoplasm resistance. Since protoplasm is a good conductor, R is much bigger than r

e.g. $R = 183$ kilo.ohm.cm

$r = 230$ ohm.cm

It may be pointed out that the above representation does not reflect the true state of affairs inside the fibre, but is based upon the 'black-box' behavior.

Before proceeding further we will define the notations in the above figure as follows:

r_m = (transverse membrane resistance/cm^2) x area of electrode at A

= $r_m \cdot a_A$ (where a_A = electrode contact area at A in cm^2)

similarly $r_b = r_m \cdot a_B$ ohm

$r_c = r_m \cdot a_C$ ohm

R_{AB} = (longitudinal membrane resistance/cm) x length of section AB(cm)

= $r \cdot \dot{\imath}_{AB}$ ohm

$R_{BC} = r \cdot \dot{\imath}_{BC}$ ohm

$C_A = C_m \cdot a_A$ microfarad; $C_B = C_m \cdot a_B$ microfarad;
$C_C = C_m \cdot a_C$ microfarad

r_{ab} = axoplasm resistance of length ab

= $r_i \cdot \dot{\imath}_{ab}$

$r_{bc} = r_i \cdot \dot{\imath}_{bc}$

If the muscle fibre is undamaged at A, B and C then

$$E_a = E_b = E_c = \text{resting potential}$$

and $$i_a = i_b = i_c = 0$$

This above equivalent circuit shows that by using suitable measuring techniques it is possible to determine the resting potential and predict the values of membrane resistance and capacitance.

These methods are described in Chapter 3.

2.4 Passive Response of Fibres

We have already stated that the muscle fibre can be con-

sidered as a single core cable. In Section 2.4 ~~and 2.4~~ we gave expressions of resistance and capacitance per unit length of such a cable. It has been observed that the muscle is not activated by currents at sub-threshold levels. Hence we can assume that the dielectric properties of the membrane material do not change when only sub-threshold currents are applied. The distribution of these currents would therefore be as shown in Figure 2.3

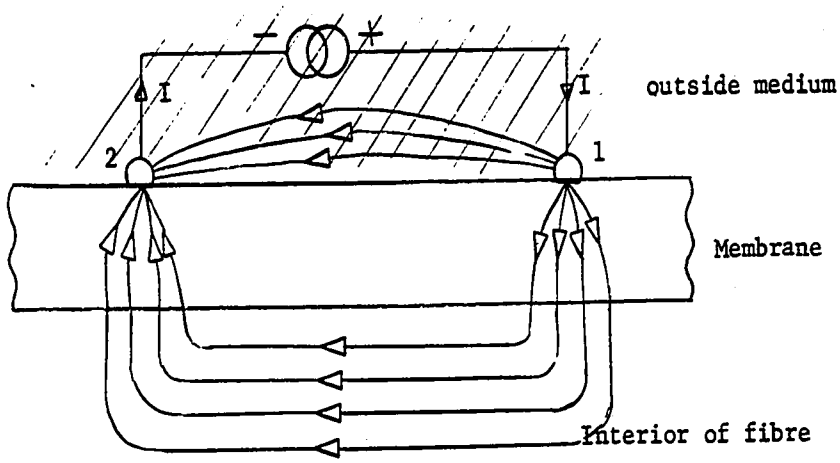

Fig.2.3

If V_m is the potential developed across the membrane due to the passage of these currents then the potential V_1 recorded externally with respect to point 1 and any other distant point '3' in the outside medium is given by

$$V_1 = \frac{r_o}{r_i + r_o} \cdot V_m$$

This would be clear from the equivalent circuit shown in Figure 2.4.

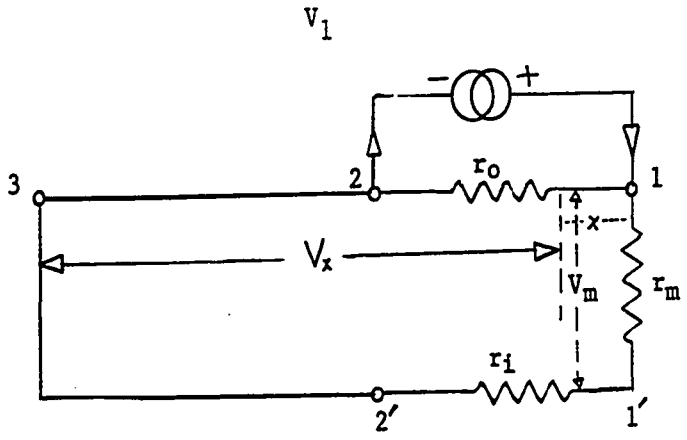

Fig. 2.4 Extrapolar region

Where

r_i is the specific resistance of protoplasm (ohm.cm)

r_o is the specific resistance of external fluid (ohm.cm)

On the basis of electric cable behavior of fibres and under the conditions outlined above Hodgkin and Rushton (42) derived expressions for calculating the passive response of nerve fibres to determine the cell constants.

The general expression derived by them for the voltage recorded between a point at distance 'x' from point 1 and a distant point in the bathing medium is given as

$$V_x = (V)_{\substack{t=\infty \\ x=o}} \frac{1}{2}\left\{ e^X \left[1+\operatorname{erf}\left(\frac{X}{2\sqrt{T}} + \sqrt{T}\right)\right] e^{-X} \left[1+\operatorname{erf}\left(\frac{X}{2\sqrt{T}} - \sqrt{T}\right)\right] \right\}$$

where $$(V_1)_{\substack{t=\infty \\ x=o}} = \frac{r_o^2 \lambda I_o}{2(r_i + r_o)}$$

$$\lambda = \sqrt{\frac{\rho_m}{r_i + r_o}}$$

I_o is a constant input current

$X = x/\lambda \qquad T = t/\tau_m \qquad \tau_m = r_m C_m$

The shape of this voltage as a function of time as observed for different values of 'x' is as shown in Figure 2.5.

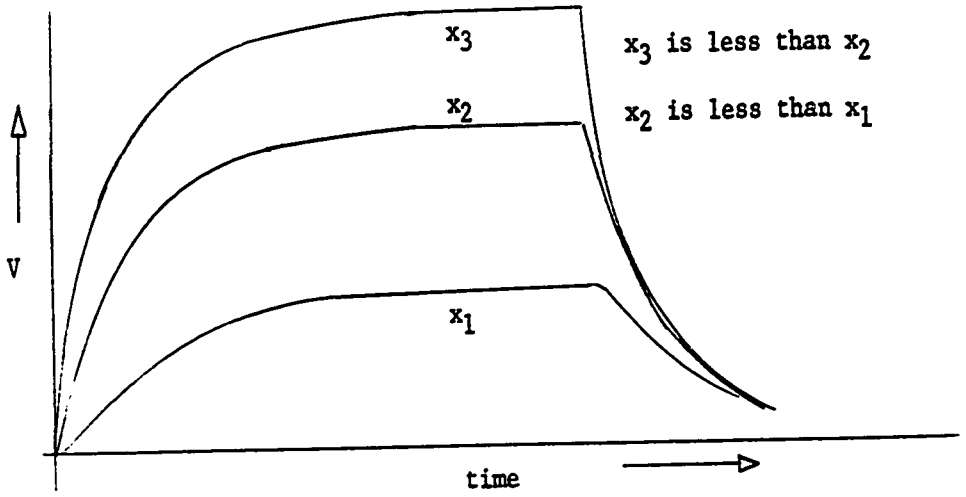

Using this formula the following average values were obtained by Katz (43) for frog muscle fibres 45 - 75 μ in diameter:

(1) Specific resistance of myoplasm about 230 ohm.cm.

(2) Transverse resistance of the fibre membrane 1500 and 4300 ohm.cm^2.

(3) Membrane capacity about 5 microfarad/cm^2.

CHAPTER 3

SUGROSE GAP METHOD

3.1 Introduction

Measurements of bioelectrical potentials with micro-electrodes present several problems. The preparation alone of these electrodes is difficult. Moreover a number of uncertainties in the measurements is introduced by the characteristics of micro-electrodes such as tip potential, junction potential and non-linear resistance. To avoid these problems an alternate technique is desirable such as the use of external electrodes. These electrodes are easy to prepare. In using external electrodes the potential difference is recorded between an intact and a depolarized portion of a muscle fibre.

If the fibre is in a fluid, there is a path short circuiting the flow of current. Under such condition the potential recorded externally would not be the actual resting potential as shown below.

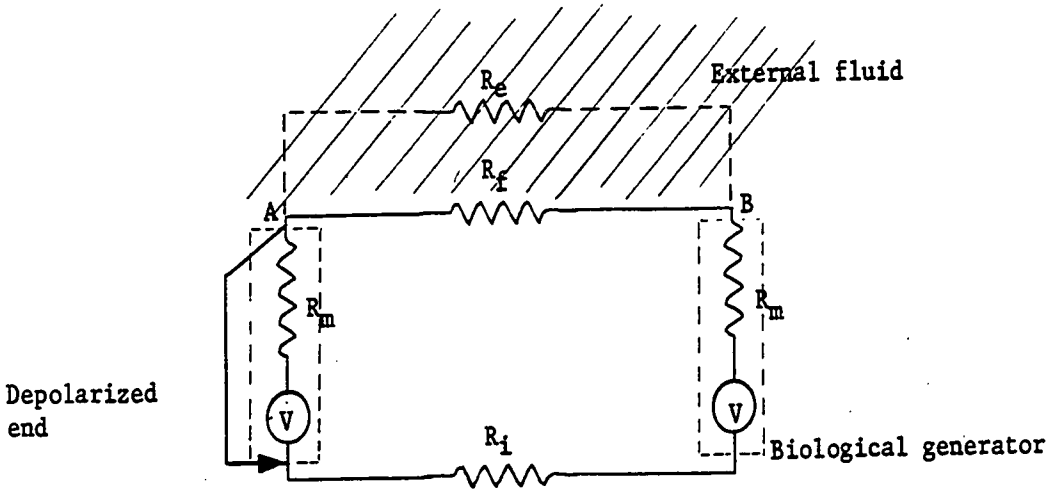

Fig. 3.1 R_f is the fibre resistance between A, B, R_m is the membrane resistance, R_i is the fibre interior resistance and R_e, the short circuiting resistance of external fluid.

From Fig. 3.1

$$V_1 = \frac{R_f}{R_i+R_m+R_f} \cdot V \quad \text{is the potential recorded externally if the fibre is not immersed in external fluid} \qquad (3.1)$$

$$= V \quad \text{for } R_f \gg (R_i+R_m)$$

$$V_2 = \frac{R_e R_f / R_e+R_f}{R_i+R_m+R_e R_f / R_e+R_f} \cdot V \quad \text{is the potential recorded when the fibre is immersed in external fluid}$$

$$= \left[\frac{R_e R_f}{(R_i+R_m)\ (R_e+R_f)\ +R_e R_f}\right] \cdot V \qquad (3.2)$$

Hence the short circuiting factor caused by external fluid

$$F_s = \frac{V_2}{V_1} = \frac{R_e R_f}{(R_i+R_m)\ (R_e+R_f)\ +\ R_e R_f} \qquad (3.3)$$

If the fluid surrounding the fibre has low specific resistance such that $R_e \ll R_f$

$$V_2 = \frac{R_e}{R_i+R_m+R_e} \cdot V$$

and $$F_s = \frac{R_e}{R_i+R_m+R_e}$$

On the other hand if the surrounding fluid has high specific resistance, such that $R_e \gg R_f$

$$V_2 = \frac{R_f}{R_i+R_m+R_f} \cdot V$$

$$= V \quad \text{for } R_f \gg (R_i+R_m)$$

and $$F_s = \frac{R_f}{R_i+R_m+R_f}$$

$$= 1 \quad \text{for } R_f \gg (R_i+R_m)$$

Huxley and Stampfli (44) obtained nearly unity short circuiting factor by immersing a single nerve fibre in medicinal liquid paraffin. The same principle was used in a different way for measuring potentials in bundles of fibres. In this case the portion between electrodes was continuously washed by isotonic sucrose solution (45). The isotonic sucrose solution (when prepared from highly purified

crystals and de-ionized) has resistivity of about 1-2 megohm. cm. Due to high resistivity of this solution it is possible to get a short circuiting factor which is very nearly unity.

Early bioelectrical measurements were done on fibres immersed in physiological solutions of low resistivity. Because of this the results were affected by the short circuiting factor. Corrections made by calculation of short circuiting factor were not satisfactory. Therefore it was felt that the 'space' or the gap between the two electrodes should be filled with some fluid of high resistivity. Thus for the portion of fibres contained in this gap we obtain a short circuiting factor nearly unity without changing the physiological state of the fibres. Since in this method an isotonic solution of sucrose is used we shall call this method a "Sucrose Gap Method" (SGM).

3.2 Measurement of Resting Potential

We will now describe the application of SGM for the measurement of resting potential in the frog toe fibres. This section contains details of a basic experiment consisting of measurement of resting potential between the intact and depolarized ends of fibres. This direct measurement does not give very accurate results due to the so called "injury current". The possibilities of improving this basic experiment by modifying the apparatus in such a way as to compensate for this current are discussed in Section 3.3. The apparatus used for our basic experiment is shown in Figure 3.2. The toe muscle fibres were tied between M1 and M2 and were supported at S1 and S2. The details of the method are as follows:

Frog toe muscle fibres were obtained from medium size frogs. The fibres were cleaned to remove the connective tissues. These fibres

APPARATUS for electrical measurements on the frog toe fibres.

(direct measurement)

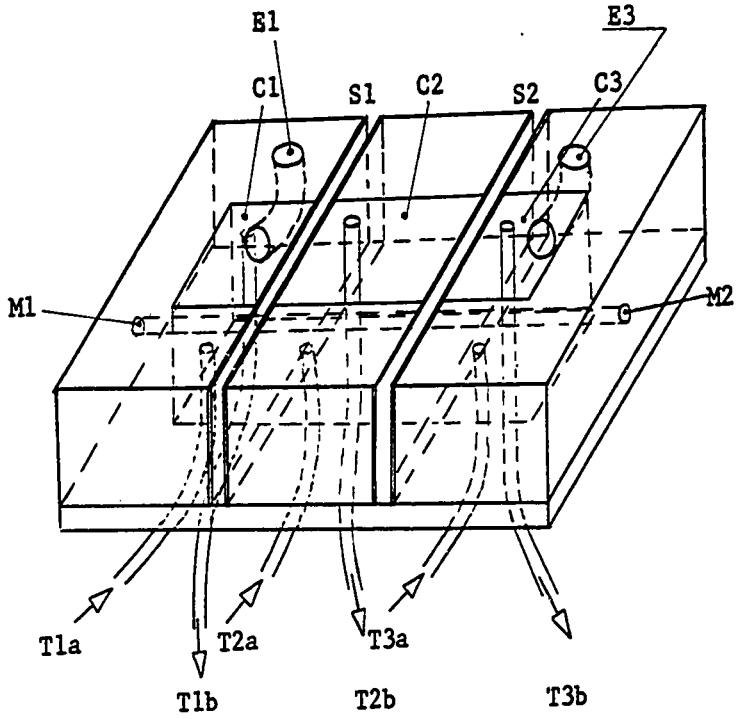

Fig. 3.2

E1,E3	seats for the AgCl-Ag-Agar electrodes
C1,C2,C3	chambers for the physiological solutions
S1,S2	spaces between chambers
M1,M2	end posts
T1a,T2a,T3a	polyethyline tubes for the continuous inflow of physiological solutions
T1b,T2b,T3b	polyethyline tubes for the continuous outflow of physiological solutions

were kept in Ringer's solution for 1-3 hours before mounting in the apparatus.

Spaces S1 and S2 were filled with petroleum jelly (Petrolatum N.F.). A uniform unidirectional flow of solutions was maintained in all three chambers to keep a constant level. The Ringer's solution was used in chambers 1 and 3 and sucrose solution in chamber 2. The two ends of muscle were tied with threads. A thread was passed with a needle through the holes for supporting the muscle, then the muscle was pulled and held between the two end holes. Two pieces of modelling clay were used both to hold the muscle and to seal the holes at the two ends. (For construction details of apparatus, the electrodes and the solutions used see Appendix 3).

The electrodes were placed in holes E1 and E3 and connected to the input of an electrometer. Measurements of resistance and potentials were taken in each of the following cases:

Case 1. Ringer's solution was used in chambers 1 and 3 and sucrose solution in chamber 2. The resistance measured between electrodes E1 and E3 was equal to the parallel resistance of fibres corresponding to the length of chamber 2. The potential difference across E1 and E3 was due to two causes:

(i) The difference in Ag-AgCl-Agar junction potential at the two electrodes.

(ii) The injury of the fibres.

Case 2. Ringer's solution was used in chamber 2 and depolarizing solution in chamber 3. The resistance measured now was the parallel resistance of axons plus the transverse membrane resistance at chamber 1 when the fibres had been fully depolarized in chamber 3. The

course of depolarization was also noted. The potential difference measured was the fibre resting potential.

Case 3. Depolarizing solution was used in chambers 1 and 3 and sucrose solution in chamber 2, thereby shorting the core conductors in these chambers. The resistance measured therefore was the parallel resistance of all the axons used. The potential recorded, if any, was due to the reason described in Case 1.

3.3 Compensation Method

When one end of the fibre is depolarized by a depolarizing solution there is a flow of current through the membrane from the unaffected end of the fibre to the depolarized end. This is shown in Fig. 3.3.

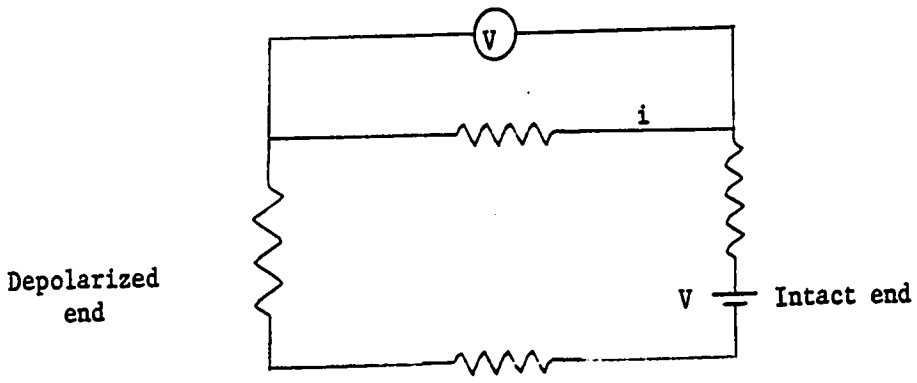

Fig.3.3

The recorded resting potential V would therefore always be less than the actual resting potential V. The current 'i' is called the membrane injury current. The error in the recorded resting potential can be eliminated by introducing a compensating network which would counterbalance the injury current thus facilitating the measurement of the actual resting potential. To achieve this the basic apparatus was modified as shown in Fig. 3.4.

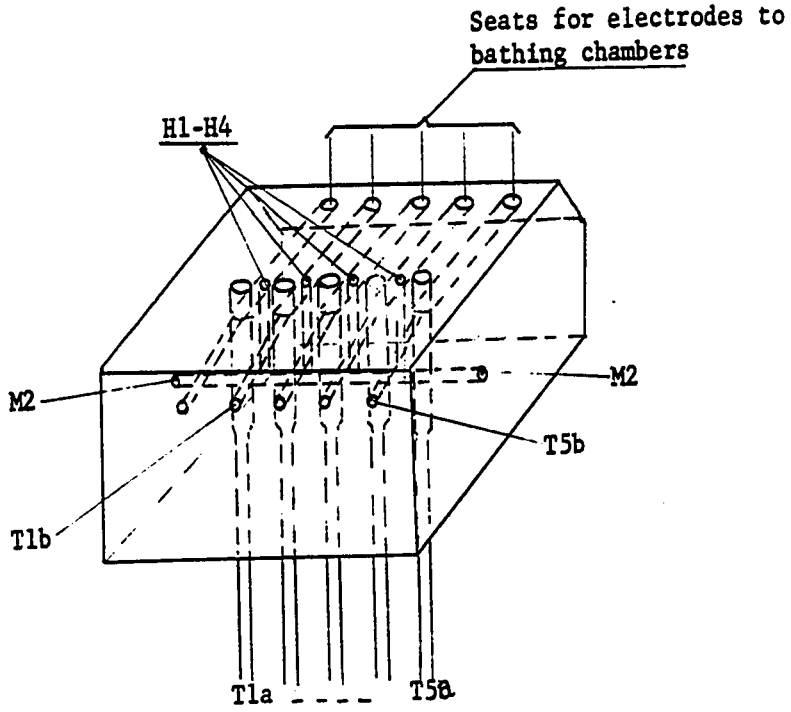

Fig. 3.4 M1-M2 ends of hole for fibres, T1a-T5a are polyethylene tubes for inflow of solutions. T1b-T5b are holes for polyethylene tubes for outflow of solutions. Small holes (shown on top between chambers) are for insulation between chambers (H1-H4).

In this apparatus, when the fibre is put in its place, extends through five chambers isolated from each other.

The compensating circuit was such as to give o-100 mv output at low conscant current. An electrometer was used as a null detector. The experimental set up is shown in Fig. 3.5.

Fig.3.5a

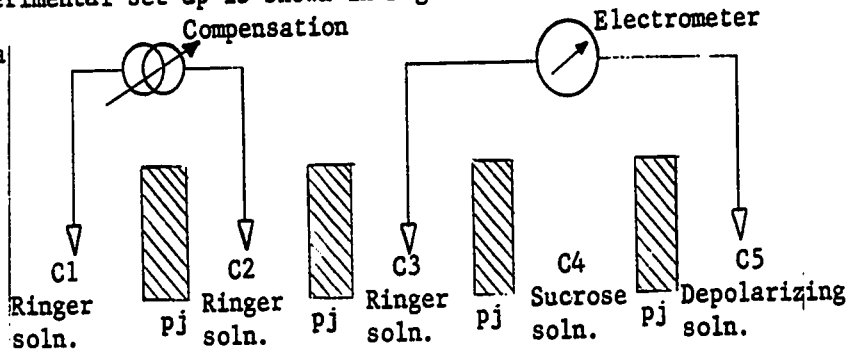

pj - Petroleum jelly seals
C - Chambers

Equivalent circuit

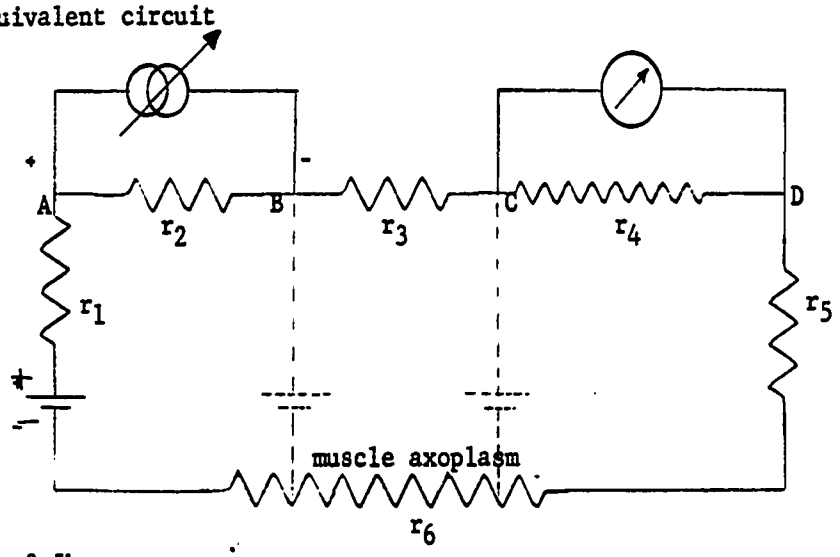

Fig.3.5b

Method: The small holes (H1 - H4) were filled with petroleum jelly. A steady unidirectional flow of solutions was maintained in all chambers. Sucrose solution was used in chamber 4 and Ringer's solution in all other chambers. The muscle was tied between the two ends by the method used before. The compensating network and the electrometer were connected as shown in Fig. 3.5 and Fig. 3.6. When the muscle was depolarized in chamber 5, a large potential difference was observed on the electrometer. This potential difference was less than the actual resting potential as discussed already.

When the compensating network was introduced and the potential difference across it was increased, the voltage across CD started

falling. The compensating voltage was further increased till $V_{cd} = o$

At this point i compensating = i injury (3.3.1)

Under this condition

$$\text{i compensating} = \frac{\text{V compensating}}{\text{parallel equivalent of } r_2 \text{ \& } (r_3+r_4+r_5+r_6+r_1)} \times \frac{r_2}{r_1+r_2+r_3+r_4+r_5+r_6}$$

but parallel equivalent of r_2 & $(r_3+r_4+r_5+r_6+r_1)$

is very nearly equal to r_2 since it is much smaller than the sum

$$(r_3+r_4+r_5+r_6+r_1)$$

Hence $$i_C = \frac{V_C}{r_1+r_2+r_3+r_4+r_5+r_6} \qquad (3.3.2)$$

Also $$\text{i injury} = \frac{V}{r_1+r_2+r_2+r_4+r_5+r_6} \qquad (3.3.3)$$

Therefore from equations (3.3.1), (3.3.2) & 3.3.3)

$V_C = V$ = actual resting potential

3.4 Experimental Results

When both ends of the muscle were immersed in Ringer's solution a small potential difference was observed across them. This potential difference, which was normally about 10 mv was attributed to the difference in junction potentials at the two Ag-Agcl-Agar electrodes and to the minor injuries in the muscle fibres. If this potential difference was 20 mv or more, the fibres were considered to be damaged and hence rejected. The toe muscles used had an average of 40 fibres, about 50 μ diameter each. An average of five readings was taken on each muscle and the time between two consecutive depolarizations was about ½ hour. The muscle was repolarized after each depolarization and was found to recover its original condition. Each preparation lasted for 3 hours or more before any significant deterioration set in. The muscle depolarization was slow until it reached a steady level. The repolarization of the muscle was more rapid when the flow of Ringer's solution was restored. Table 3.1 gives average values measured on five toe muscle preparations on different days.

TABLE 3.1

Preparation	Length of muscle fibre between electrodes cm	Resting Potential mv without compensation	Resting Potential mv with compensation	Resistance when both ends in Ringer's MΩ	Resistance when one end depolarized MΩ	Resistance when both ends depolarized MΩ
1	1	75	82	2.81	3.8	3.0
2	1	70	79	2.2	3.6	2.9
3	1	67	-	2.1	3.5	2.6
4	1	78	82	2.8	3.9	2.8
5	1	77	82	2.4	3.8	2.8
Average	1	73.2	84.7	2.46	3.72	2.82

Discussion of Results

Ideally the compensation circuit counterbalances the injury current and the measured resting potential approaches actual resting potential of the fibre. However this is strictly true in case of myelinated nerve fibres only, where the current flows across the membrane at the nodes of Ranvier. In this case the fibre between two nodes is covered by an insulating sheath (myelin) as shown in Fig. 3.6a. The current flows from one node (the unaffected) to the other node (the depolarized one) and there is no current flow across the membrane between the two nodes. But in case of muscle fibre the biological generator units are spread along the length and the current flows across the membrane at all points and is directed towards the

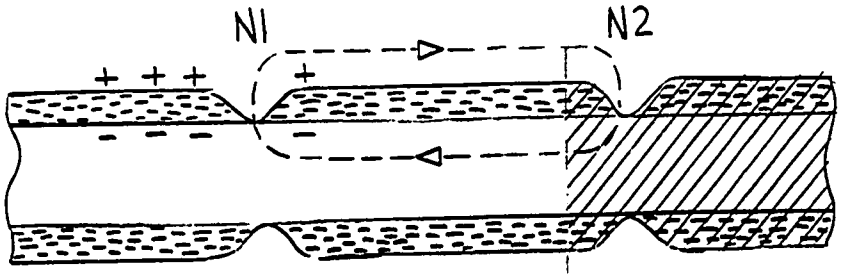

Fig.3.5a Nerve fibre: N1 and N2 are nodes of Ranvier

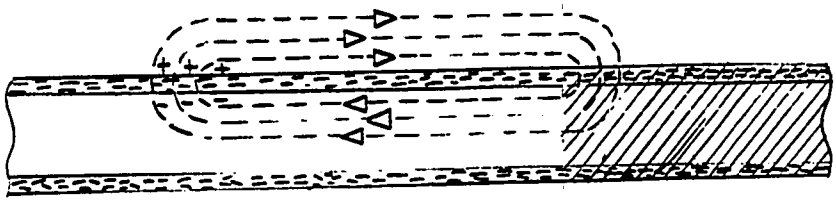

Fig.3.5b Muscle fibre

Depolarized end

depolarized end following the path of the least resistance. Total injury current is therefore the sum of these currents. Therefore resting potential estimated from the amount of compensation tends to be higher than the actual resting potential of the fibre. Thus the recorded resting potential before and after compensation would differ by a large amount. This effect was observed in our experiment. (Appendix 4)

CHAPTER 4

NEUTRALIZED INPUT CAPACITY PREAMPLIFIER FOR BIOLOGICAL RESEARCH

Bioelectrical potentials are the potentials which appear across the membranes in living cells. These potentials can be measured in a number of ways depending upon the type of cells. In measurements on frog sartorious fibres the muscle is immersed in Ringer solution* and a microelectrode is inserted very carefully in a single fibre to measure the potential appearing across the membrane. The signal from the microelectrode is amplified and measured with a suitable instrument (eg. CRO).

Figures 4.1 and 4.2 show the physical arrangement and the apparatus used in such measurements.

The resistance of microelectrodes ranges from a few megohms to tens of megohms (see Appendix 5). This resistance combined with the microelectrode capacitance to ground and the capacity of the input stage give a large time constant (RC). The "cut-off" frequency of the input circuit expressed in terms of the time constant

$$f_i = \frac{1}{2\pi RC}$$

In a typical case

$R = 10M\Omega$ $\quad C = 20$ Pf

Hence

$$f_i = \frac{1}{6.28 \times 10^{7} \times 20 \times 10^{-12}}$$

$$= 0.8 \text{ KC/S}$$

---

* A solution resembling blood serum in its salt constituents

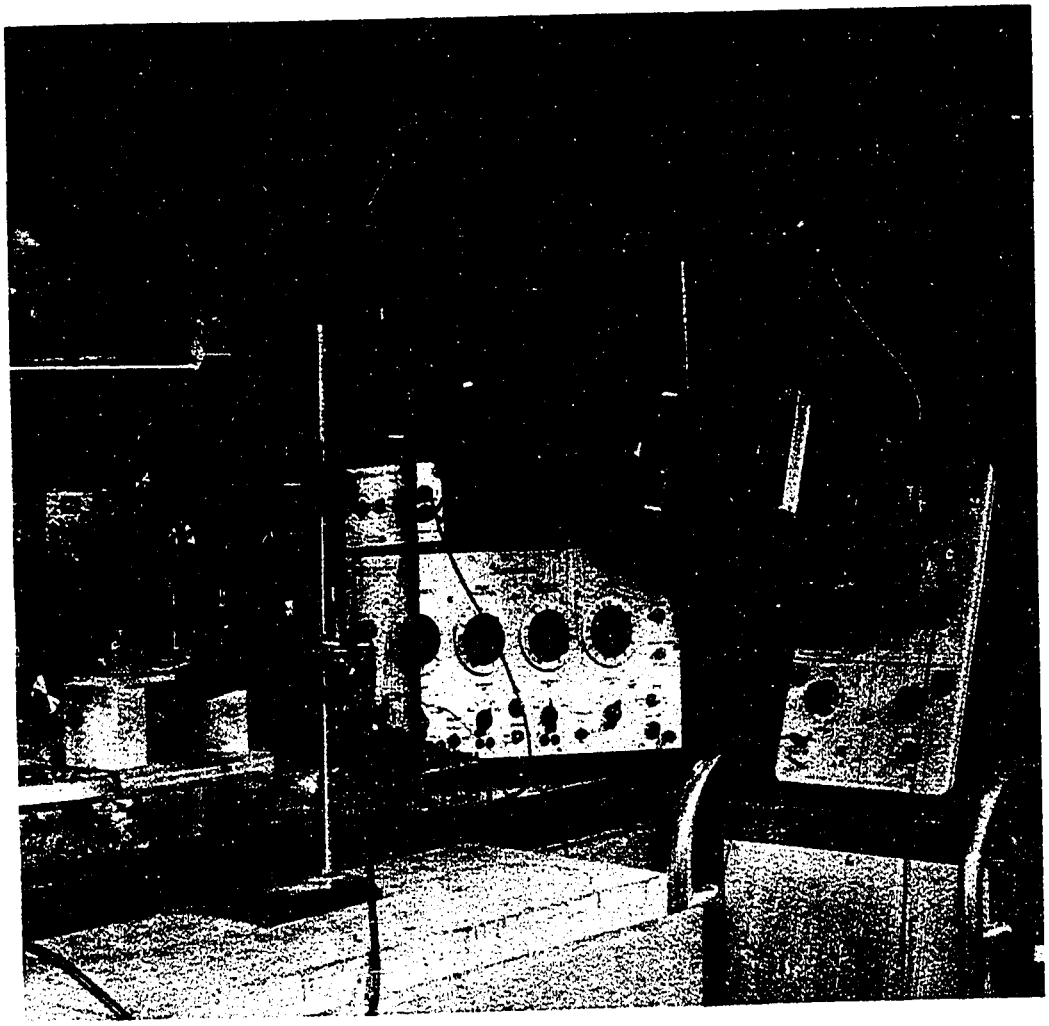

Figure 4.1

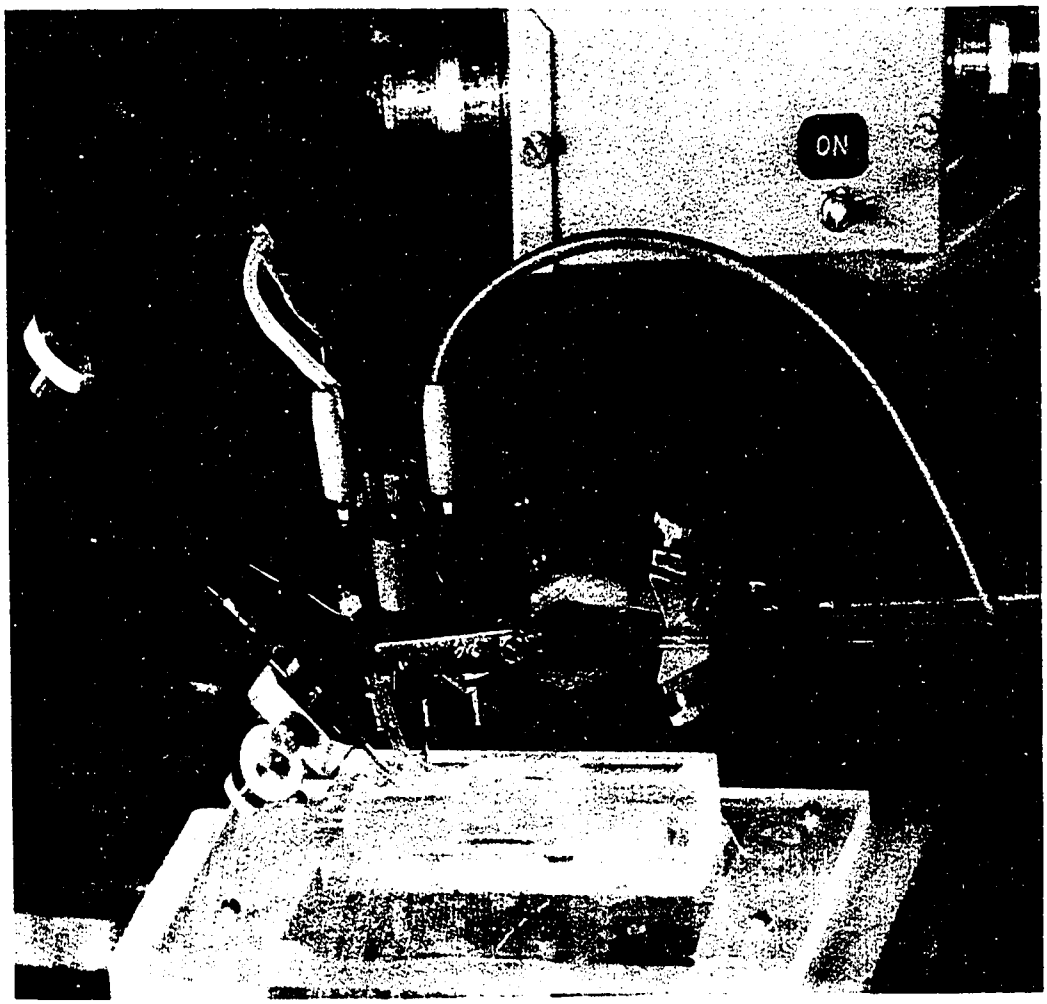

Figure 4.2

The bioelectrical potentials resulting from excitation, called action potentials, of nerve cells or muscle fibres have rising phase as short as 100 microseconds (46) whereas the after potentials* may last for many seconds. Therefore for faithful reproduction of these potentials the frequency response of the preamplifier should extend from dc to at least 30kc**.

There are also other factors which influence the design of the preamplifier.

(1) The current flowing through the specimen should be less than 10^{-9} ampere.

(2) Because of the high resistance at the input precautions have to be taken against the pick-up from stray fields.

An electrometer tube is a natural choice for the input stage of the preamplifier because of its very low grid current (10^{-10}-10^{-15} ampere.)

---

* These are negative and positive potentials of very low magnitude which appear after the main spike and are believed to be associated with metabolic changes occurring inside the cells.

** A 100 microseconds duration of the rising phase of action potential corresponds to a fundamental frequency of about 3kc/s. By extending the frequency response to 30kc/s, the response will include more harmonics hence better reproduction of the wave form. The figure of 30kc/s is thus an arbitrary one and in general the wider the bandwidth the less distortion of the wave-form. Since an increase in bandwidth also increases noise, the bandwidth of the amplifier has to compromise these two conflicting factors.

The pick-up from stray fields can be minimized by enclosing the apparatus and the preamplifier in a well grounded screen. The 60 cps ripple can be eliminated by using batteries for supplying the power to the preamplifier. Because of the practical considerations the first requirement calls for a small size and the second for a low power consumption and these can be easily realized by using transistors as amplifying elements.

In order to extend the frequency response of the input stage its time constant (RC) has to be made shorter. Since the reduction of microelectrode resistance gives rise to undesirable problems, the only factor which can be changed is the input capacitance. There is a number of methods of reducing the effective capacitance of the input circuit, one of which being the use of positive feedback through a capacitance (47, 48, 49, 50).

A transistorized preamplifier using an electrometer tube was developed at the Columbia University in 1956 (51).

This design has been adopted in the work as a starting point for further modifications to achieve

(1) ease of adjustment and single point control

(2) economy in size, so that the preamplifier could be mounted as close to the preparation as convenient. (The dimensions are 4" x 2-1/4" x 2-1/4")

(3) saving in cost

(4) improvement in performance

The equivalent circuit of this amplifier (circuit diagram, Fig. 4.15)

is shown in Fig.4.3, where C_g is the input capacity at amplifier input terminals including microelectrode capacitance to ground; C_f is the feed back capacitance

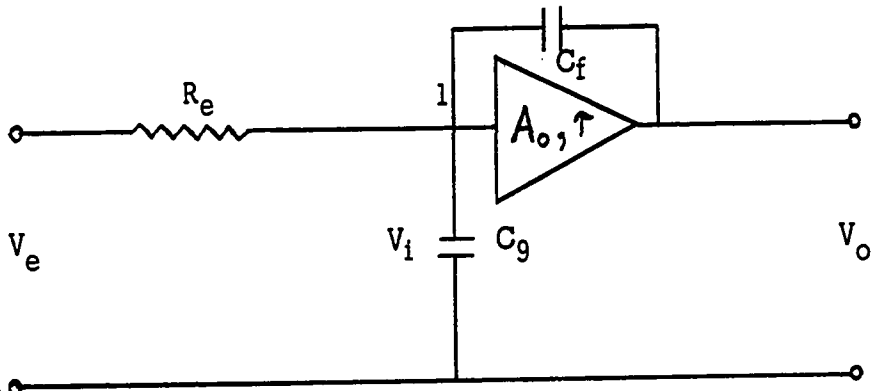

Fig. 4.3

If the amplifier is characterized by low frequency gain A_o and the time constant τ , then it can be shown that the equivalent input circuit capacitance with feedback

$$Ceq. = C_g + C_f (1-A_o) + \frac{\tau}{R_e} \qquad (4.1)$$

Under these conditions if $A_o \gg 1$, C_{eq} can be reduced to zero by a suitable adjustment of the feedback capacitance C_f.

However in practice the equivalent capacitance at the input is only reduced to a certain minimum finite value. This is because the microelectrode is composed of distributed parameters and the lumped parameter representation has been adopted for convenience in analysis. Fig. 4.4 shows equivalent circuit of a typical experimental arrangement (52)

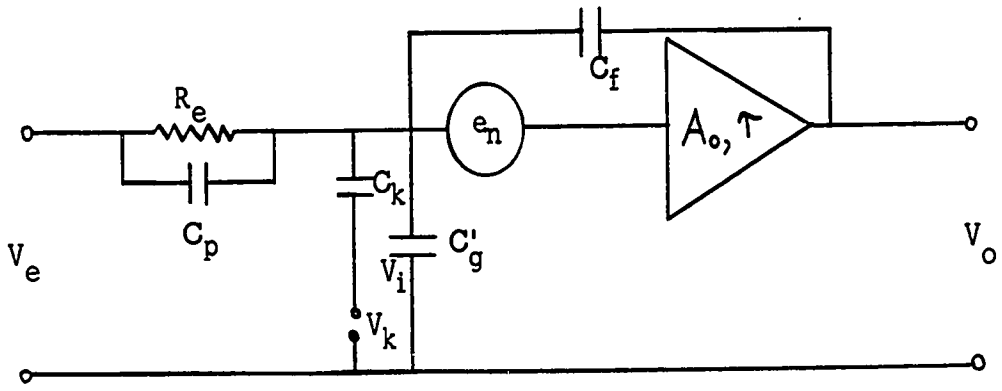

Fig. 4.4

R_e = microelectrode resistance

C_p = parallel cpacitance of microelectrode

C_k = capacitance of microelectrode with respect to elevated potential V_k above ground

C'_g = input terminal capacitance of the amplifier

V_i = input signal

e_n = equivalent noise of the amplifier circuit

V_e, V_i, V_o are the Laplace transforms of the corresponding time functions $v_e(t)$, $v_i(t)$ and $v_o(t)$

For calculating the response of the amplifier, we will make use of Fig.4.3. Writing current equations for node 1

$$\frac{V_e - V_i}{R_e} - V_i S C_g - (V_i - V_o) S C_f = 0 \qquad (4.2)$$

but
$$V'_o = A' V_i = \frac{A_o}{1+S\tau} V_i \qquad (4.3)$$

$\therefore$ from (2) $\frac{V_e - V_o(1+S\tau)}{R_e} - V_o(1-S\ )C_g - \left[V_o(1+S\tau) - A_o V_o\right] S C_f = 0$

$$V_e - V_o \left[1 + S\left\{\tau + R_e(C_g + C_f - A_o C_f)\right\} + S^2 \left\{ R_e(C_g + C_f)\right\}\tau \right] = 0$$

Setting $R_e (C_g + C_f - A_o C_f) + \tau = \alpha T$

and $2\sqrt{(C_g + C_f) R_e \tau} = T \qquad (4.4)$

$$\frac{V_o}{V_e} = \frac{1}{1 + S\alpha T + S^2 (\frac{1}{2}T)^2} \qquad (4.5)$$

The response is a second order function characterized by time the constant 'T' and damping factor 'α'

$$V_e = V_o \left[1 + S\alpha T + S^2 (\tfrac{1}{2}T)^2\right]$$

In time domain

$$V_e(t) = V_o(t) + \alpha T \frac{d}{dt} v_o(t) + 1/4T^2 \frac{d^2}{dt^2} v_o(t) \qquad (4.6)$$

For a step input 'E'

$$1/4T^2 \frac{d^2}{dt^2} v_o(t) + \alpha/T \frac{d}{dt} v_o(t) + v_o(t) = E \qquad (4.7)$$

The characteristic roots of the left hand side of this equation are $2/T \left[-\alpha \pm \sqrt{\alpha^2-1} \right]$

Therefore the differential equation gives three types of solutions for $v_o(t)$ depending upon the value of 'α'

(i) When $\alpha = 1$, there is one double root equal to $-2/T$. In this case

$$\frac{v_o(t)}{E} = 1 - (1+2t/T) \text{ Exp } (-2t/T) \qquad (4.8)$$

and the response is as shown in Fig. 4.5 curve 'a'

(ii) When $\alpha > 1$, there are two real roots. In this case

$$\frac{v_o(t)}{E} = 1 - \frac{1}{b-a} \left\{ b \text{ Exp} \left(\frac{-2at}{T}\right) - a \text{ Exp} \left(\frac{-2bt}{T}\right) \right\} \qquad (4.9)$$

where $a = \alpha - \sqrt{\alpha^2-1}$

$b = \alpha + \sqrt{\alpha^2-1}$

and the response is as shown in Fig. 4.5 curve 'b'

(iii) When $\alpha < 1$, the roots are complex and conjugate. In this case

$$\frac{v_o(t)}{E} = 1 \frac{1}{1-\alpha^2} \text{ Sin} \left\{ \sqrt{1-\alpha^2} \frac{2}{T} t + \phi \right\} \text{Exp}\left(-\frac{\alpha^2}{T} t\right) \qquad (4.10)$$

where $\tan \phi = \frac{\sqrt{1-\alpha^2}}{\alpha}$

and the response is as shown in Fig. 4.5 curve 'c'

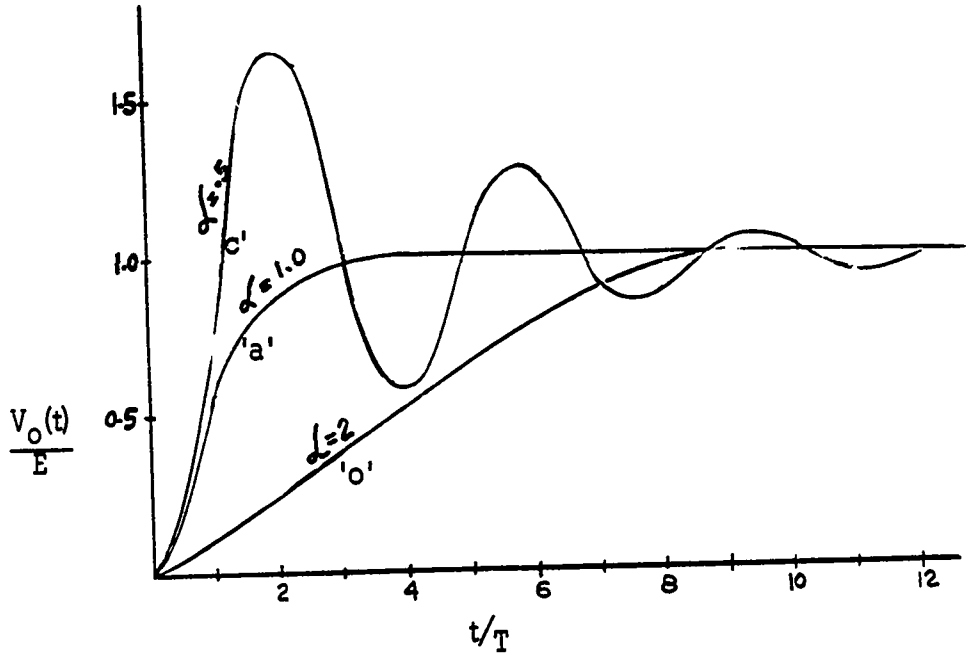

Fig. 4.5

EXPERIMENTAL RESULTS

Measurements have been made on an experimental set up as shown in Fig. 4.6. The following curves were obtained

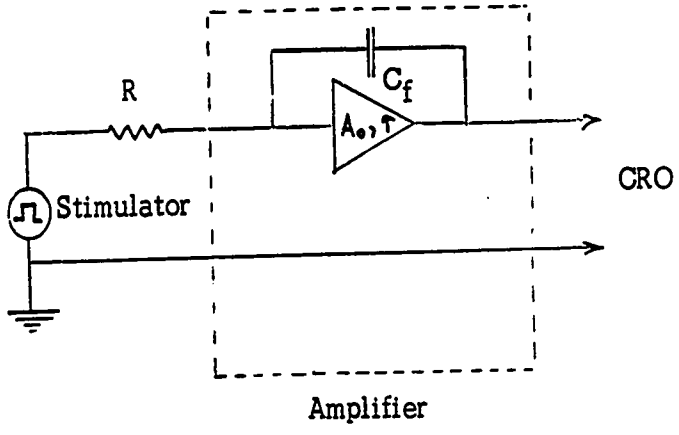

Fig. 4.6

Figure 4.7: 200 microseconds pulse through 10 megohms resistor

Bottom trace 'b', : Minimum value of C_f, maximum damping $\alpha > 1$

Middle trace 'a', : Optimum compensation for minimum rise time $\alpha = 1$

Top trace 'c', : Over compensation, oscillatory response $\alpha < 1$

Figure 4.8: 200 microseconds pulse through 22 megohms resistor

From Figure 4.7, the equivalent time constant is estimated to be (less than) 2 microseconds. Therefore, the value of equivalent RC product

$= 2 \times 10^{-6}$ sec.

$R = 10$ megohms $= 10^7$ ohms

Hence, effective capacitance after neutralization,

$$= \frac{2 \times 10^{-6}}{10^7} = 0.2 \text{pf}$$

The frequency response of the system with feedback

$$f_i = \frac{1}{2\pi RC}$$

$$= \frac{1}{2\pi \times 2 \times 10^{-6}} = 80 \text{kc/s}$$

Charging current can be estimated as

$$i_c = C_{eq} \frac{dv_o(t)}{dt}$$

taking $\frac{dv_o(t)}{dt} = 10^3$ v/sec.

$$i_c = 0.2 \times 10^{-12} \times 10^3$$

$$= 0.2 \times 10^{-9} \text{ amp.}$$

$$= 1/5 \text{ nano amp.}$$

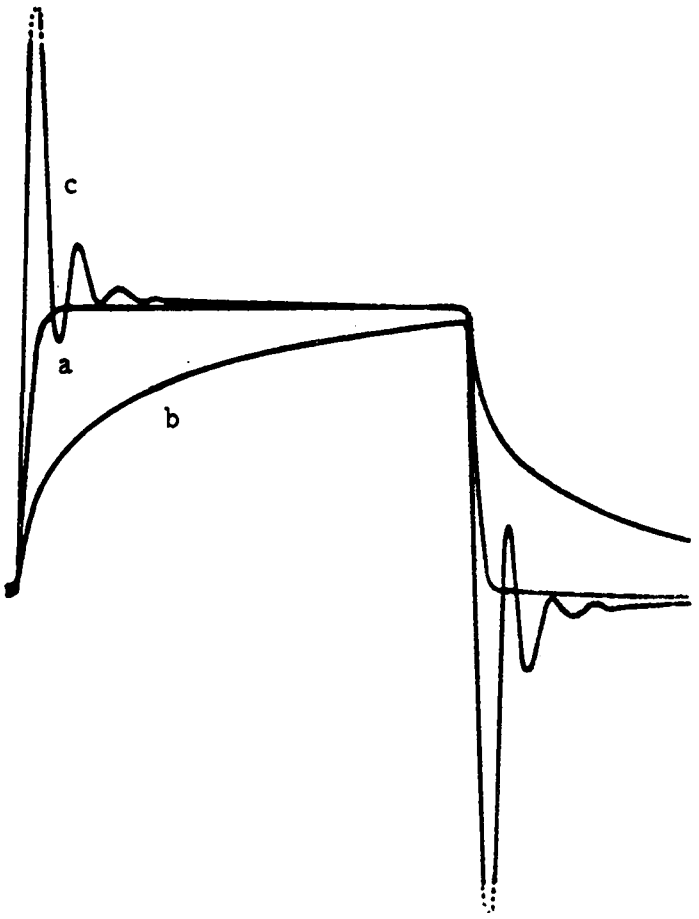

Figure 4.7

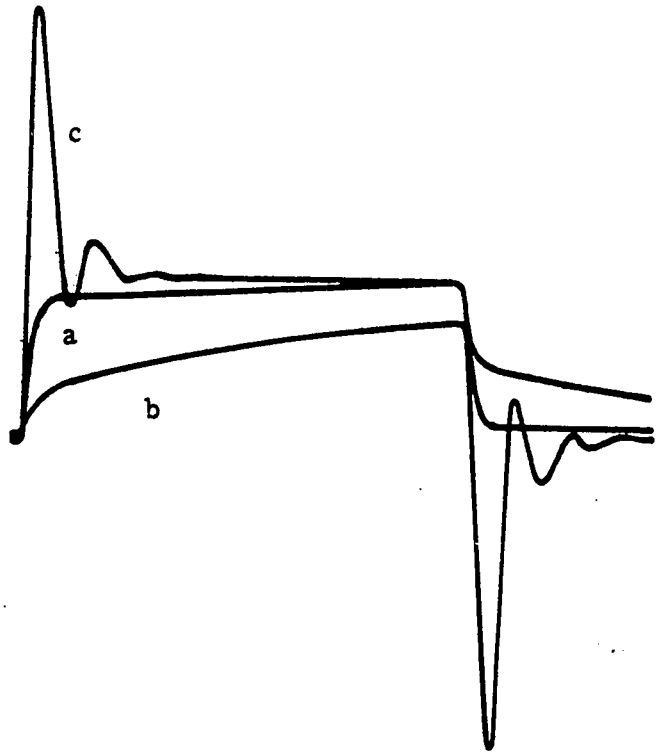

Figure 4.8

Curves b, a, c are CRO traces obtained by triple exposure. Trace 'c' corresponds to C_f = 7 pf. The value of C_f was then increased to obtain 'a'. A further increase in C_f causes oscillations as shown in 'c'.

The above experiment was repeated with 10 megohms microelectrode. The set up was as shown in Fig. 4.9. Figure 4.10 shows typical curves obtained. There is striking difference between the oscillatory responses in the two cases. This is because the microelectrode capacitance with respect to the immersing fluid is not grounded. Changing the arrangement of Fig. 4.9 to Fig. 4.11 curves similar to the ones in Figures 4.7 & 4.8 were obtained.

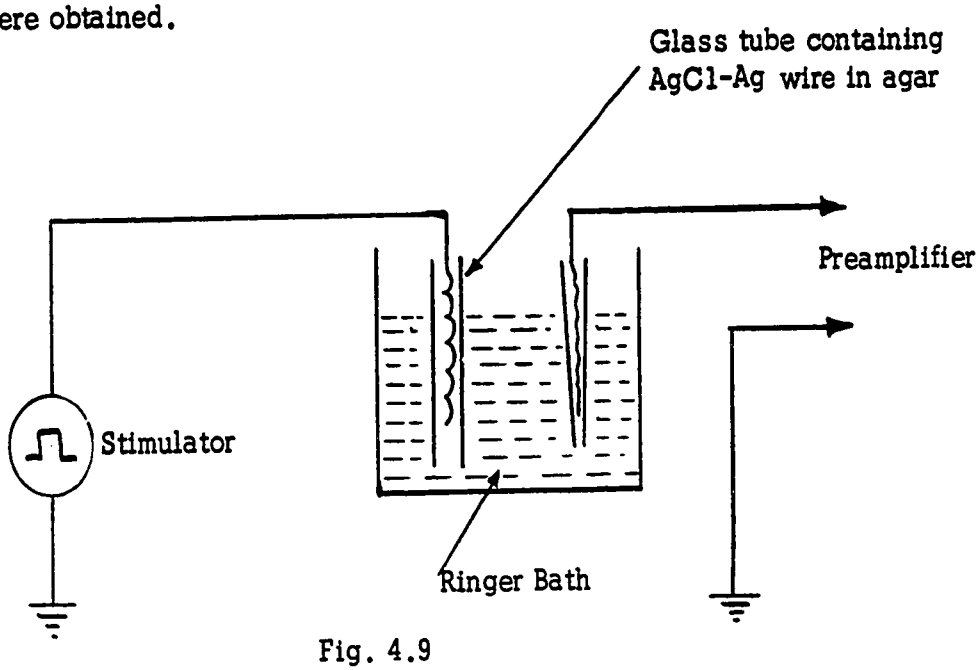

Fig. 4.9

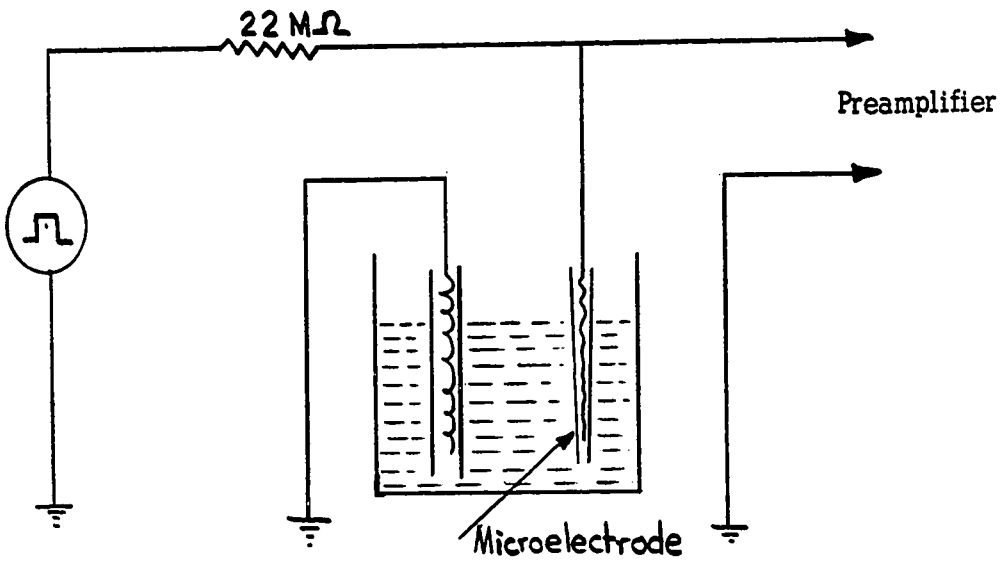

Fig. 4.11

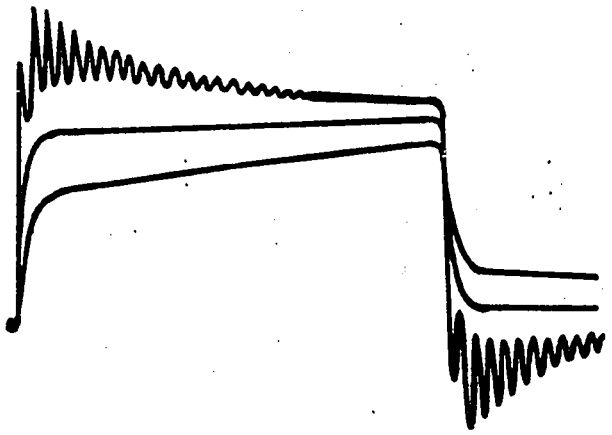

Figure 4.10. Preamplifier response for the three cases of compensation (triple exposure). The experimental set - up is shown in figure 9.

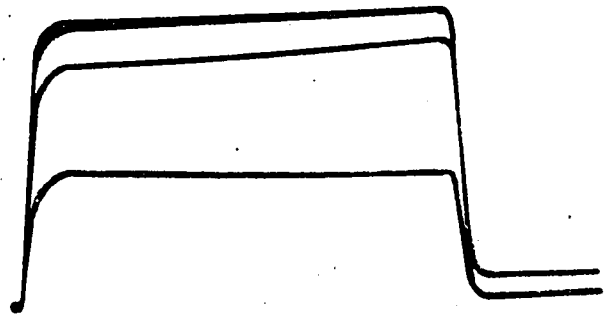

Figure 4.12. CRO traces for the experiment shown in figure 13. The values of resistances connected for traces from top to bottom 10MΩ, 22MΩ, 80MΩ and 200MΩ respectively.

Figure412 shows four different curves obtained by connecting resistances of 10 megohms, 22 megohms, 80 megohms, and 200 megohms consecutively, at the input. (Fig. 4.13).

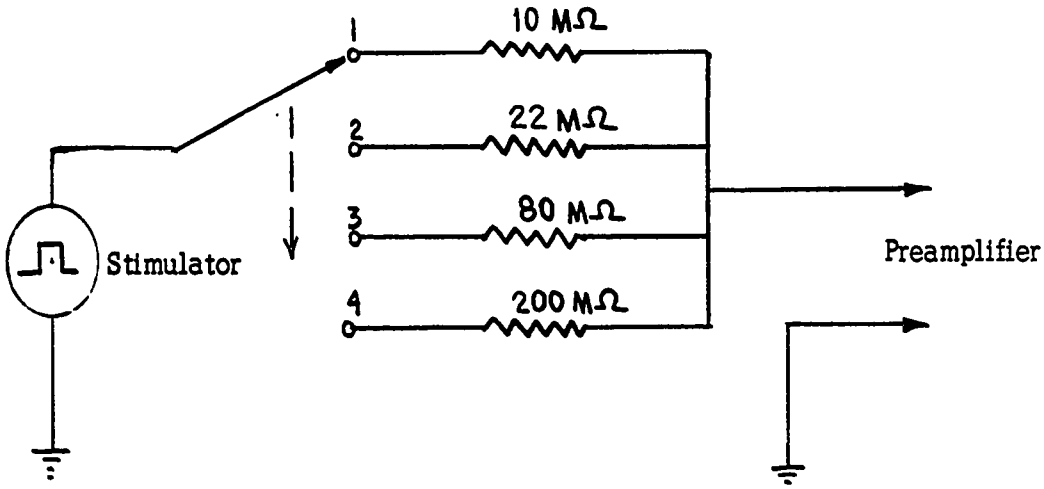

Fig. 4.13

The curves for 10 megohms and 22 megohms practically overlap.

Attenuation factor corresponding to 80 megohms

$$\frac{R_{in}}{R + R_{in}} = 0.9$$

Where R_{in} = Input impedance of the amplifier

= 9R = 720 megohms

Input current may be estimated as

$$i = \frac{\Delta E}{\Delta R}$$

for curves 2 and 3

ΔE = 10mV

ΔR = 70 megohms

$i = 10^{-2}/70 \times 10^{6} = 1.4 \times 10^{-10}$ Amp.

NOISE

The available noise power from a signal source is defined as the maximum power that can be delivered to an external load connected across it.(53) Fig.4.14. This maximum occurs when the load resistance is equal to the source resistance.

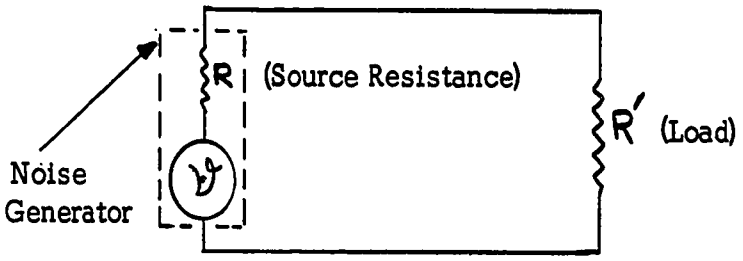

Fig. 4.14

Therefore, power delivered to R' $= \left[\frac{\overline{v^2}}{R+R'}\right]^2 R'$

and $R = R'$, $P = P_a$

i.e. available noise power $= \frac{\overline{v^2}}{4R}$

According to Nyquist Theorem,

$$\overline{v^2} = 4kTR\,df \qquad (4.11)$$

where k = Boltzman constant = 1.38×10^{-23} j $(^\circ K)^{-1}$

T = Abs. temp ($^\circ$K)

df = small range of frequencies

Hence RMS noise voltage $\sqrt{\overline{v^2}} = 2\sqrt{kTR\ df}$

In a typical case

R = 10 MΩ $\qquad$ df = 80 kc

Therefore rms noise voltage

= 115 microvolts.

This noise level is not significant when recording action potentials which are of the order of 100 mV.

CONCLUDING REMARKS

The microelectrode has high resistance. The effective resistance of microelectrode and membrane may fluctuate during an experiment. Therefore high input resistance of the preamplifier is useful for reducing inaccuracies in the recorded signal due to these changes.

The purpose of the above experimental analysis of the preamplifier was to evaluate its characteristics which are important in bioelectrical measurements.

There is not sufficient data available on other amplifiers used in biological research, on their behavior under experimental conditions. Therefore it is hard to make a quantitative comparison. The values of input current, input impedance and frequency response as obtained in the experiment show that these values conform to basic requirements in bioelectrical measurements.

By proper choice of electrometer tube and transistors the frequency response of the preamplifier can be extended without generating much noise in the circuit. The noise introduced by the feedback path can be neglected over the useful range. The high frequency response of the amplifier is useful for accurate reproduction of action potentials. Where the input signals are either d.c. or slowly varying potentials, the bandwidth can be reduced. Reduction in bandwidth reduces noise and makes it possible to measure signals in the microvolt range.

This preamplifier is being used at the Physiology Department of the University of Ottawa, for recording resting and action potentials in frog toe and sartorious fibres. A study of these records will be useful for

making further improvements in the present design.

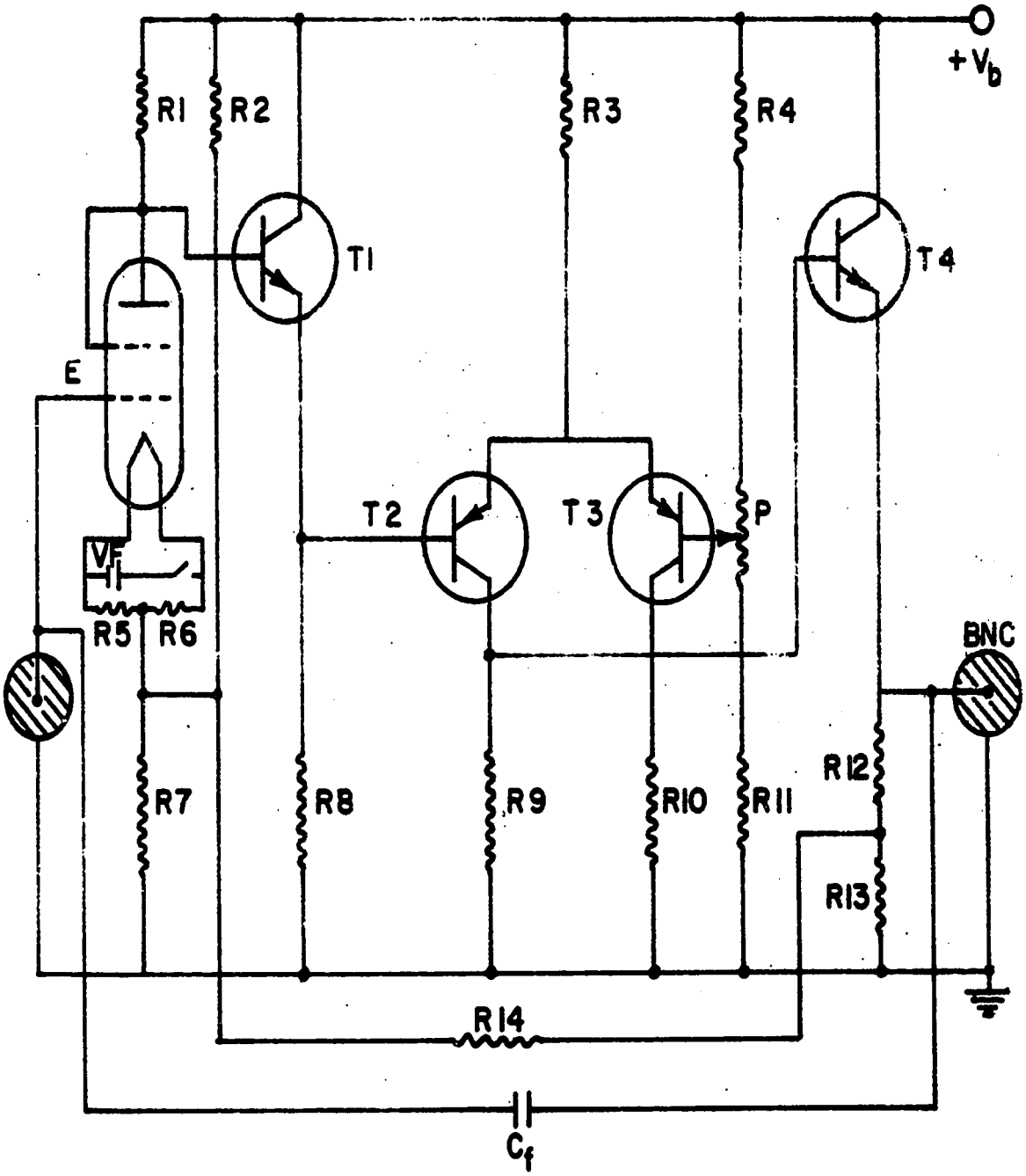

Figure 4.15

R1,R9,R10	12K	R14	270 ohms
R2	8.2K	P	Potentiometer 500Ω
R3	2.7K	Cf	7-45 Pf
R4	1K	E	Electrometer tube 5886
R5,R6	470 ohms	T1,T4	Transistors 2N 1306
R7	1.8K	T2,T3	Transistors 2N 1307
R8,R11	5.6K	Vb	16-8 volts
R12,R13	2.2K	Vf	1-35 volts

CHAPTER 5

MICROELECTRODES

5.1 Introduction

Living tissues e.g., muscle fibres and nerve cells have microscopic dimensions. The frog toe and sartorious fibres are about 50 - 100 μ in diameter. The microelectrodes for puncturing the membrane of these fibres have to be much smaller in diameter so that physical injury does not change fibre characteristics.

There are two general types of microelectrodes used in bioelectrical measurements (54, 55).

1. Metal electrodes or metal filled pipette electrodes.
2. Fluid filled pipette electrodes.

The choice between these two types is determined not by convenience but by the type of electrical measurement required.

For the purpose of analysis an electrode may be represented by its electrical equivalent consisting of a resistance 'R' and capacitance 'C' (See Fig. 5.1).

Consequently the electrical activity in the cells is transmitted to the measuring instrument through a network whose frequency characteristic depends on the value of RC.

Metal filled electrodes have low resistance, thereby having a better frequency response than the fluid filled ones. However when the metal comes in contact with a medium containing charged ions, there is a formation of a double layer of ions which behaves like a capacitor. This would modify the electrical equivalent of the probe from that in Fig. 5.1(b) to the one shown in Fig. 5.2.

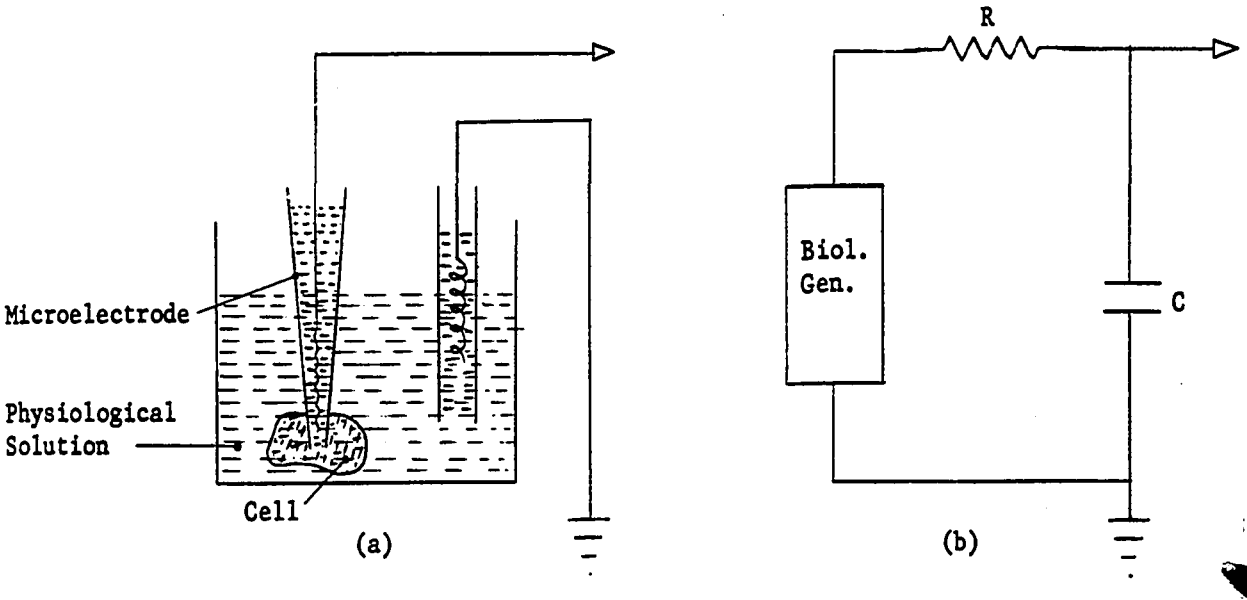

Fig. 5.1 R is the microelectrode resistance (or fluid resistance) inside the micropipette mainly concentrated near the tip. C is the capacitance between the fluid filling the micropipette and the immersing solution. The connection to the micropipette fluid is made by immersing AgCl-Ag wire in it.

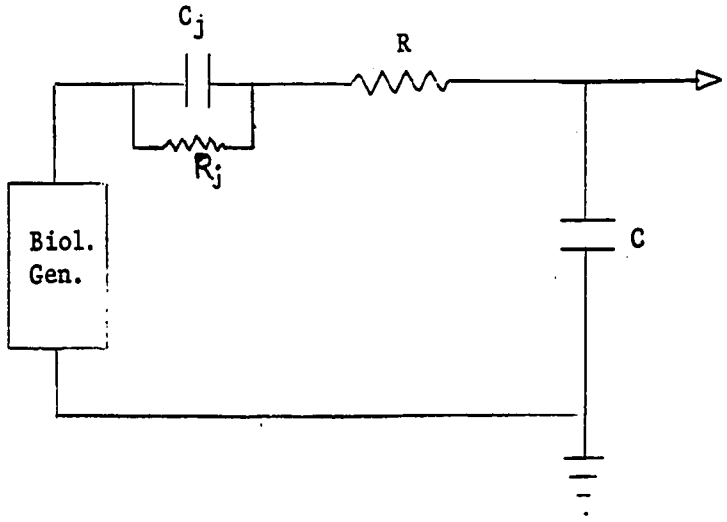

Fig. 5.2 C_j represents capacitance at the junction of two media of different ionic concentrations.

Because of the appearance of the capacitance C_j, the slow changes inside the cell would not be recorded on the measuring instrument. The junction potential at the tip of these electrodes has irregular variations, thus making them undesirable except for recording rapid variations.

The fluid filled electrodes have high resistance, hence poor frequency response. However they would record slow variations and the junction potential at the tip of these electrodes is constant depending on the ionic concentrations. The frequency response of these electrodes can be improved by the technique described in Chapter IV.

The electrolytic solution used to fill these electrodes was in our case 3M KCl solution and this choice has been made for the following reasons:

(1) K^+ and Cl^- ions have similar mobilities and hence the tip potential is steady.

(2) The high concentration reduces diffusion potentials due to other ions and the junction currents are largely carried by K^+ and Cl^-.

(3) The high concentration KCl solution has lower specific resistance, therefore the microelectrodes of small tip diameter filled with 3M KCl would not have very high resistance.

During measurements diffusion of ions from the tip into the cell can change the ionic content of the cells. The amount of diffusion from an electrode having an external tip diameter 0.4μ and filled with 3M KCl solution is 6×10^{-14} moles per sec. (56). This rate of diffusion of KCl into the cells would not cause any appreciable change in muscle fibres.

The electrical connection from the electrolyte of such an electrode to the measuring instrument is made by inserting in KCl solution a silver (Ag) wire deposited with AgCl.

5.2 Preparation of fluid filled microelectrodes

The machine used for production of microelectrodes is the same as described by Winsbury (57). The main electrode puller assembly is shown in Figure 5.3.

The glass capillary is held between the two pin vices. To the lower pin vice is attached a 'plunger' through a steel rod. The glass tube is heated by a heating coil surrounding the tube. When, due to heating, the tube becomes plastic, it extends by the gravitational pull of the plunger and the steel rod. When the tube is extended a solenoid is energized at a pre-set point exerting a heavy downward pull on the plunger. In this way two electrodes are produced simultaneously.

Dimensions of microelectrodes i.e., tip diameter, shank slope and length of the shank are governed by the following parameters:

(i) temperature of the heating coil,

(ii) length of the first pull (before the solenoid is energized),

(iii) magnitude of solenoid pull exerted on the plunger.

If the temperature of the heating coil is too high, the resulting electrodes have either very small tips or closed tips. At low temperatures the tip diameter produced is large.

The length to which the tube is extended during the first pull governs the shank slope. When this length is small the slope is large and for greater length the slope is small.

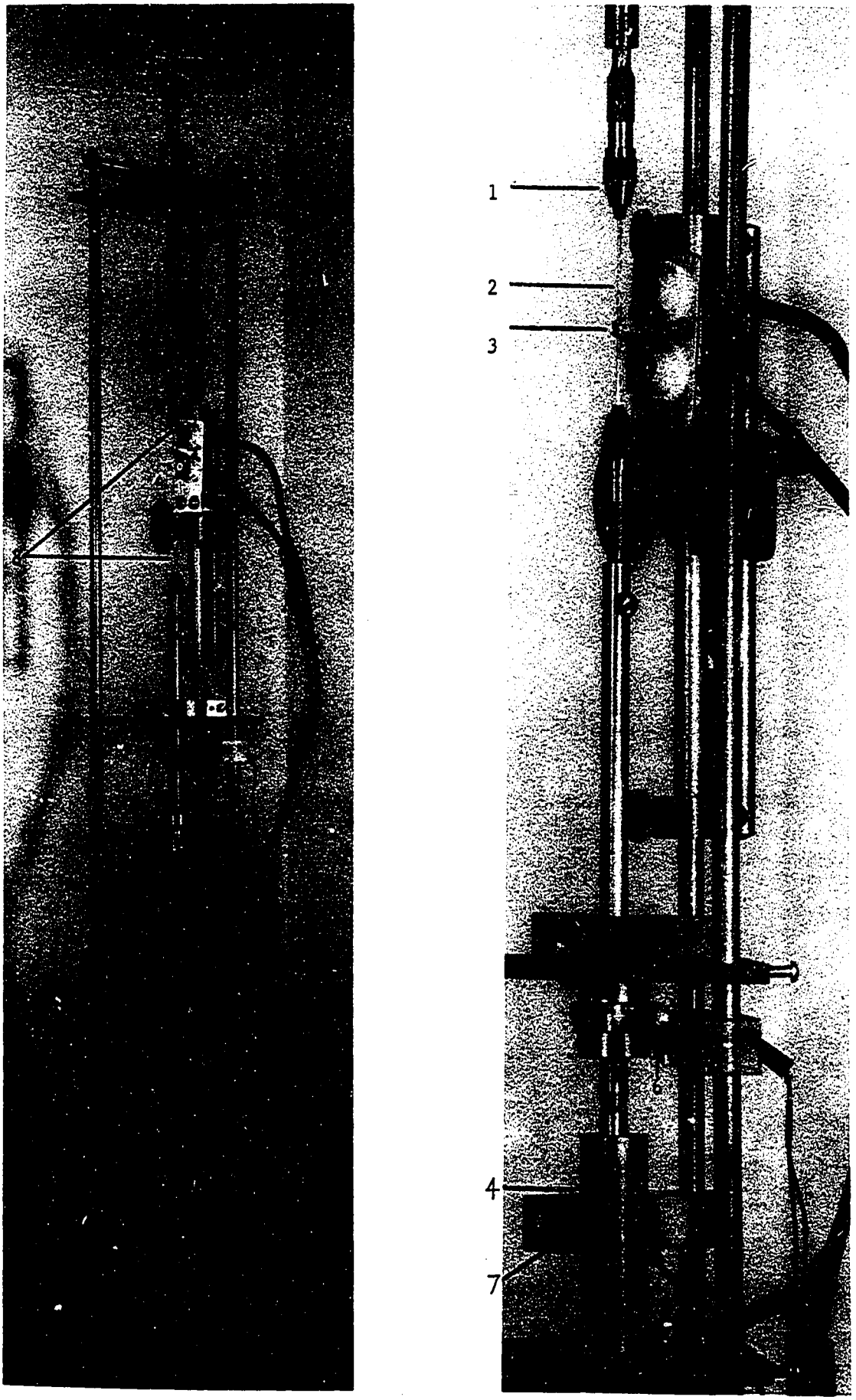

Fig. 5.3: Machine for the production of microelectrodes
(1) Pin Vice (2) Glass Tube (3) Heating Coil (4) Plunger
(5) The length to which the tube (when it becomes plastic) is extended under the gravitational pull before the solenoid is energized (6) Solenoid actuating microswitch (7) Master microswitch. (8) Microelectrodes

When the solenoid pull on the plunger is very strong, the tip diameter tends to be small and the tips may break. If this pull is too small the diameter would be too large.

We used heating coil made of 3 turns of platinum wire .052" in diameter. The coil diameter was 0.25".

Fig. 5.4 shows the circuit diagram of the heating and solenoid elements.

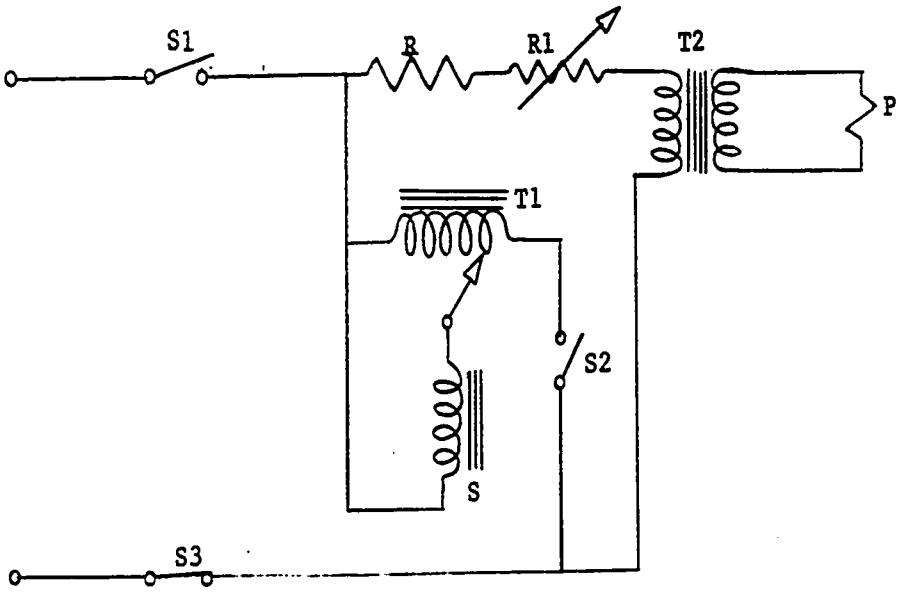

Fig. 5.4 Circuit diagram of microelectrode machine.
S1, on/off switch; S2, solenoid actuating microswitch;
S3, master microswitch; R, R1 fixed and variable
resistances for controlling heating coil current;
T1, T2 kva variac; T2 coil transformer 230/3.3V;
S, solenoid; P, platinum coil.

For the minimum value of R1, the heating coil current started at 82 amps. and dropped down to 46 amperes as the coil temperature reached about 700°C. The terminal to terminal resistance of the coil was 8.5 milliohms when cold and 26.2 milliohms at 700°C. Under these conditions the length of the first pull for tubes of smaller

diameter was 12 sec. and 16 sec. for tubes of larger diameter and thicker glass.

For maximum value of 'R', the coil current started at 71 A and dropped down to 42 A at coil temp. as before. In this case the lengths of the first pull for the two cases mentioned above was found to be 15 sec. and 22 sec. respectively.

The useful range of solenoid pull on the plunger was found to be 40 to 60% of its maximum value.

Data for microelectrodes obtained for medium positions of 'R', and medium solenoid pull are given below. The values of resistances given were measured as described below on the probes filled with 3M KCl solution and immersed in Ringer's solution.

TABLE 5.1

No.	Resistance
1	12.5 MΩ
2	6.6 "
3	5.0 "
4	5.2 "
5	12.0 "
6	21.0 "
7	3.4 "
8	15.5 "
9	13.6 "
10	6.2 "
Average value of resistance	10.1 "

5.2.2 Filling of Microelectrodes

After pulling, the electrodes were examined under a high power optical microscope (x1000) to check if the tips were not broken or closed and whether the tip diameter was in the desired range.

They were then fastened onto a glass slide by a rubber band. The slide was immersed in a glass jar containing dust free methanol with the electrode tips pointing downwards. The glass jar was placed in a vacuum and the pressure was reduced until methanol started boiling. The air in electrodes was displaced by methanol which filled the electrodes completely in a few minutes. The glass slide with the probes was then transferred to another glass jar filled with dust free distilled water. The electrodes were kept there for a minimum of 12 hours so that distilled water filled the probes and displaced methanol. Finally these probes were transferred to a 3M KCl solution. The KCl solution displaced distilled water and filled the electrodes. A period of 6 hours was allowed for this final stage to ensure complete displacement of distilled water by KCl solution. After this the electrodes were considered to be ready for use.

5.2.3 Measurements on Microelectrodes

A simplified arrangement used for measuring resistance and tip potential of microelectrodes is shown in Fig. 5.5.

When switch 'S' is open, the potential difference measured between points 2 and 3 was the electrode tip potential.

The switch 'S' was then closed and 100 mv, 1 KC pulses were passed through the circuit shown.

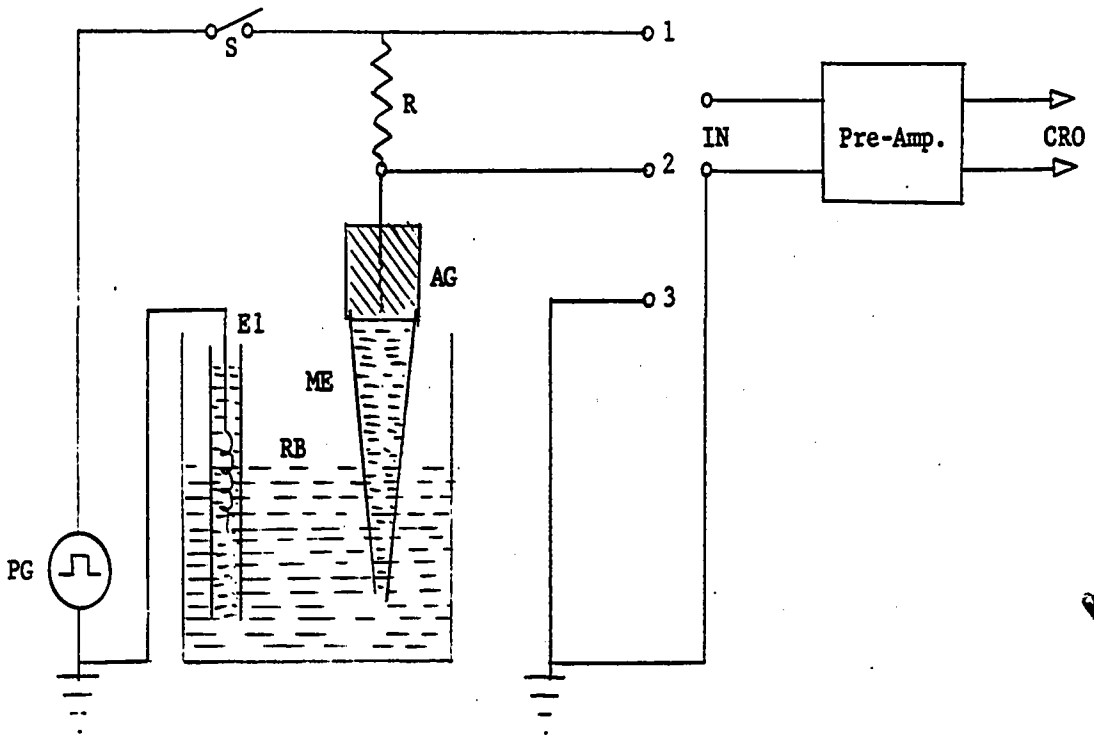

Fig. 5.5 RB, Ringer's solution bath; E1, Ag-AgCl-Agar electrode; ME, microelectrode filled with 3M KCl solution; AG, agar bridge containing AgCl-Ag wire; S, switch for connecting pulse generator (PG) to the microelectrode; R, 10-20 M resistance.

If V_{13} and V_{23} is the potential measured between points (1 and 3) and (2 and 3) respectively, the resistance of microelectrode

$$R_e = \frac{V_{23}}{V_{13} - V_{23}} R \qquad (5.2.3.1)$$

5.3 Analysis of Microelectrodes

In Appendix 5, we derived an expression for the equivalent resistance of fluid-filled glass microelectrode. This is given as

$$R_{eq} = \frac{1}{\pi d} \left[2 \rho_{in} (\tan \phi)^{-1} + \rho_{out} \right]$$

where

ρ_{in} is the specific resistance of fluid used for filling the microelectrode.

ρ_{out} is the specific resistance of physiological solution in which the microelectrode is immersed when its resistance is measured.

$\tan \phi$ is the slope of the shank of microelectrode.

d is the internal tip diameter of microelectrode.

We have plotted the calculated values of this resistance in Fig. 5.6, taking

ρ_{in} = 3.36 Ωcm. for 3M KCl solution

ρ_{out} = 82 Ωcm. for Ringer's solution

The ordinates give the values of Req in megohms, the abcissae give internal tip diameter in microns and different curves have been obtained for different values of $\tan \phi$.

It can be seen that Req is an inverse function of the internal tip diameter and of the shank slope.

If the tip diameter is large, a big electrode resistance would only be obtained for very small slopes. This tends to make the electrode shank longer. An electrode with a long shank tends to break and is not strong enough to puncture the cell membrane. A very small tip diameter for the same resistance would have very small shank length and again would not be useful for measurements on cell membrane.

It can be seen from the curves that a microelectrode would have, theoretically, a resistance of about 10 MΩ for the following combinations of the diameter and slope:

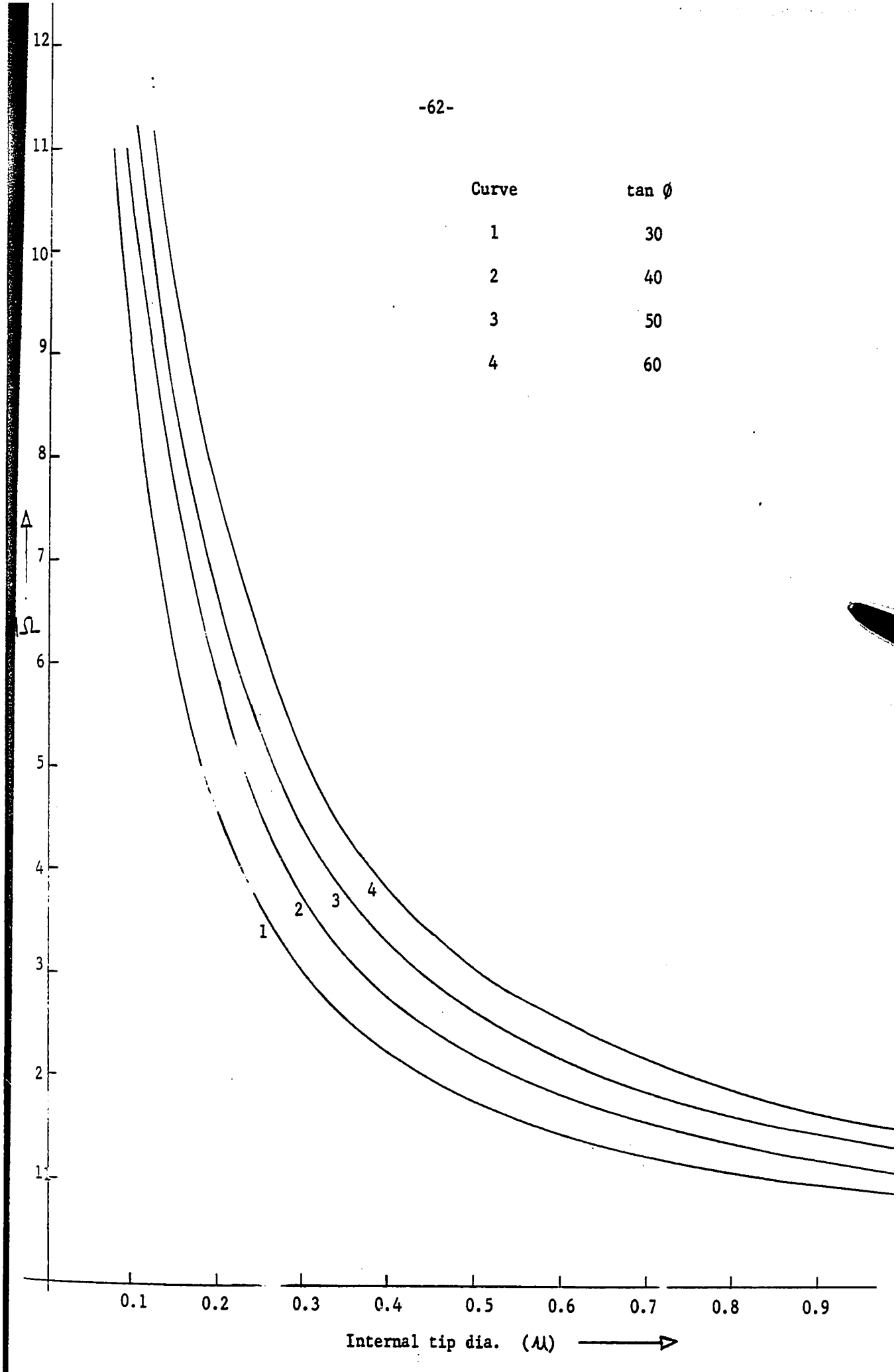

Fig. 5.6 Calculated values of microelectrode resistance.

Internal Tip Dia. (μ)	Slope tan ϕ
0.10	1/35
0.111	1/40
0.122	1/45
0.133	1/50
0.144	1/55
0.155	1/60

It can be seen that for such submicroscopic dimensions the use of optical microscopes for the purpose of analysis or selection of microelectrodes is inaccurate.

We carried out two main experiments for comparing the theoretical values of resistance with those measured experimentally:

(1) When the electrodes selected were of larger ($>0.3\mu$) diameter and lower ($<5M\Omega$) resistance.

(2) When the electrodes selected were of smaller ($<0.3\mu$) diameter and higher resistance ($>5M\Omega$).

In the first case, the coil heat and solenoid pull were adjusted so as to give electrodes of 0.5 to 1.0μ tip diameter. Pictures of these electrodes were taken by an optical microscope at a magnification of x720. The electrodes were then filled with 3M KCl solution by the method already described. The pictures of microelectrodes were used to measure tip diameter and shank slope. These values were substituted in the formulae

$$R_1 = \frac{1}{\pi d}\left[\, 3.36\ (\tan \phi)^{-1} + 3.36 \,\right] \quad \Omega$$

$$R_2 = \frac{1}{\pi d}\left[\, 3.36\ (\tan \phi)^{-1} + 82 \,\right] \quad \Omega$$

where

R_1 is the microelectrode resistance filled with 3M KCl solution and immersed in 3M KCl solution.

R_2 is the microelectrode resistance filled with 3M KCl solution and immersed in Ringer's solution.

The corresponding values were determined experimentally. The data obtained is given in Table 5.2.

TABLE 5.2

Electrode	Estimated Dimensions		Calculated Resistance		Measured Resistance	
	d μ	$(\tan \phi)^{-1}$ -	R_1 megohm	R_2 megohm	R_1 megohm	R_2 megohm
1	0.62	25.6	0.9	1.2	0.6	1.8
2	0.87	35.7	0.88	1.06	0.86	1.6
3	0.46	39.5	1.86	2.4	1.40	2.3
4	0.63	25.8	0.87	1.29	0.82	1.40
5	0.35	35.6	2.2	2.92	1.92	3.20
6	1.34	35.9	0.58	0.79	0.63	0.72

(b) In the second part of the first case we prepared some electrodes and filled them with 3M KCl. After measuring the electrode resistance, these were washed with distilled water and a few were selected for further measurements under the electron microscope. Their dimensions were thus measured and the resistance calculated. Table 5.3 shows the results obtained.

TABLE 5.3

GROUP I Prepared from bigger dia.glass tubes at low heat and 55% max. pull of solenoid. (Note: Low and high heat correspond to the two values of heating coil currents discussed in Section 5.2.)

	Electrode	Measured Resistance MΩ
	1	2.6
	2	3.5
	3	3.2
*	4	2.8

Electron micrograph results

Code	Electrode	$(\tan \phi)^{-1}$	d	Calculated Resistance
145	4	23	0.35 μ	2.15 MΩ

Note: The code refers to no. of electron microgh shown in Fig. 5.7 and Fig. 5.8.

TABLE 5.3

GROUP II Prepared from smaller dia. glass tubes at low heat and 50% of maximum solenoid pull.

	Electrode	Resistance MΩ
	1	7.5
	2	1.8
	3	3.6
	4	3.2
*	5	2.4
**	6	2.5
	7	2.6
	8	14.5
	9	3.3
	10	3.9

Electron micrograph results

Code	Electrode	$(\tan \phi)^{-1}$	d (μ)	Calculated Resistance (MΩ)
149	5	30	0.45	2.0
151	6	25	0.40	2.0

In the second case we tried to adopt a statistical approach to compare the measured resistance of microelectrodes. In this case a few electrodes were selected at random from each batch of electrodes prepared and photographed under an electron microscope. The remaining electrodes were filled with 3M KCl solution and their resistance was measured while immersed in Ringer's solution.

GROUP I: Prepared from small diameter glass tubes, at about 50% of maximum solenoid pull and low heat.

Electrode	Resistance MΩ
1	3.8
2	13.0
3	4.4
4	6.0
5	4.9
6	2.0
7	2.5
Average	5.17

Sample electron micrograph results

Code	$(\tan \phi)^{-1}$	d (μ)	Calculated Resistance (MΩ)
140	41	0.25	4.6
141	42	0.25	4.65
142	40	0.50	2.20
Average	41	0.33	3.82

GROUP II: Prepared from small diameter glass tubes at 50% of maximum solenoid pull and low heat.

Electrode	Resistance (MΩ)
1	4.5
2	5.6
3	7.0
4	5.5
5	5.7
6	9.0
7	14.0
8	15.0
9	7.0
Average	8.14

Sample electron micrograph results

Code	$(\tan \phi)^{-1}$	d (μ)	Calculated Resistance (MΩ)
133	36	0.4	2.58
135	42	0.3	3.87
Average	39	0.35	3.22

GROUP III: Prepared from bigger diameter glass tubes at about 60% of maximum solenoid pull and high heat.

Electrode	Resistance (MΩ)
1	24
2	19
3	6
4	17
5	10
6	9.5
7	6.2
8	15.0
Average	13.3

Sample electron micrograph results

Code	$(\tan \phi)^{-1}$	d (μ)	Calculated Resistance (MΩ)
125	45	0.15	8.17
128	48	0.20	6.44
129	47	0.40	3.16
Average	47	0.25	5.92

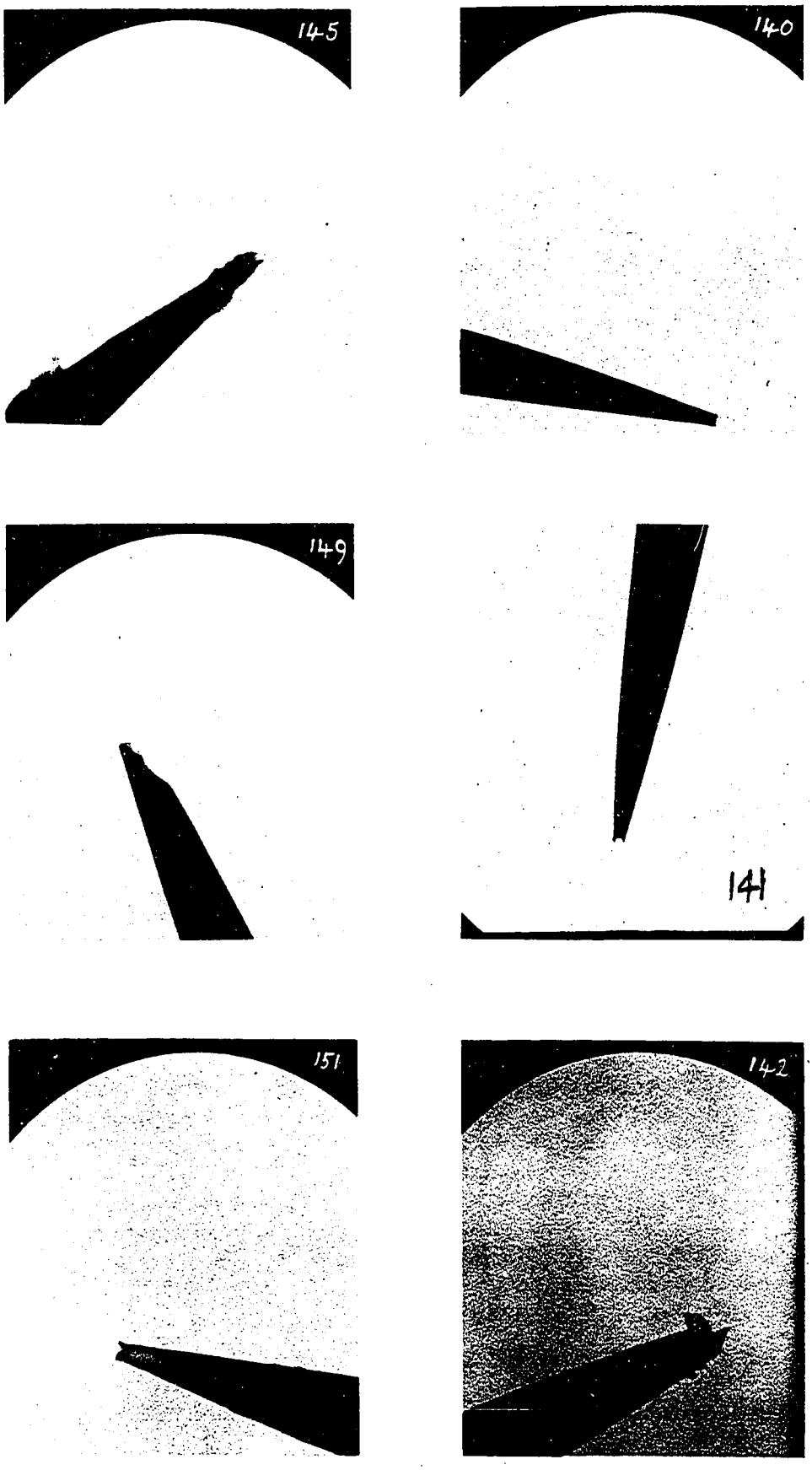

Fig. 5.7 Electron micrographs of microelectrodes (x7000)

(Courtesy of Dr. M. Colonnier, Department of Anatomy, University of Ottawa)

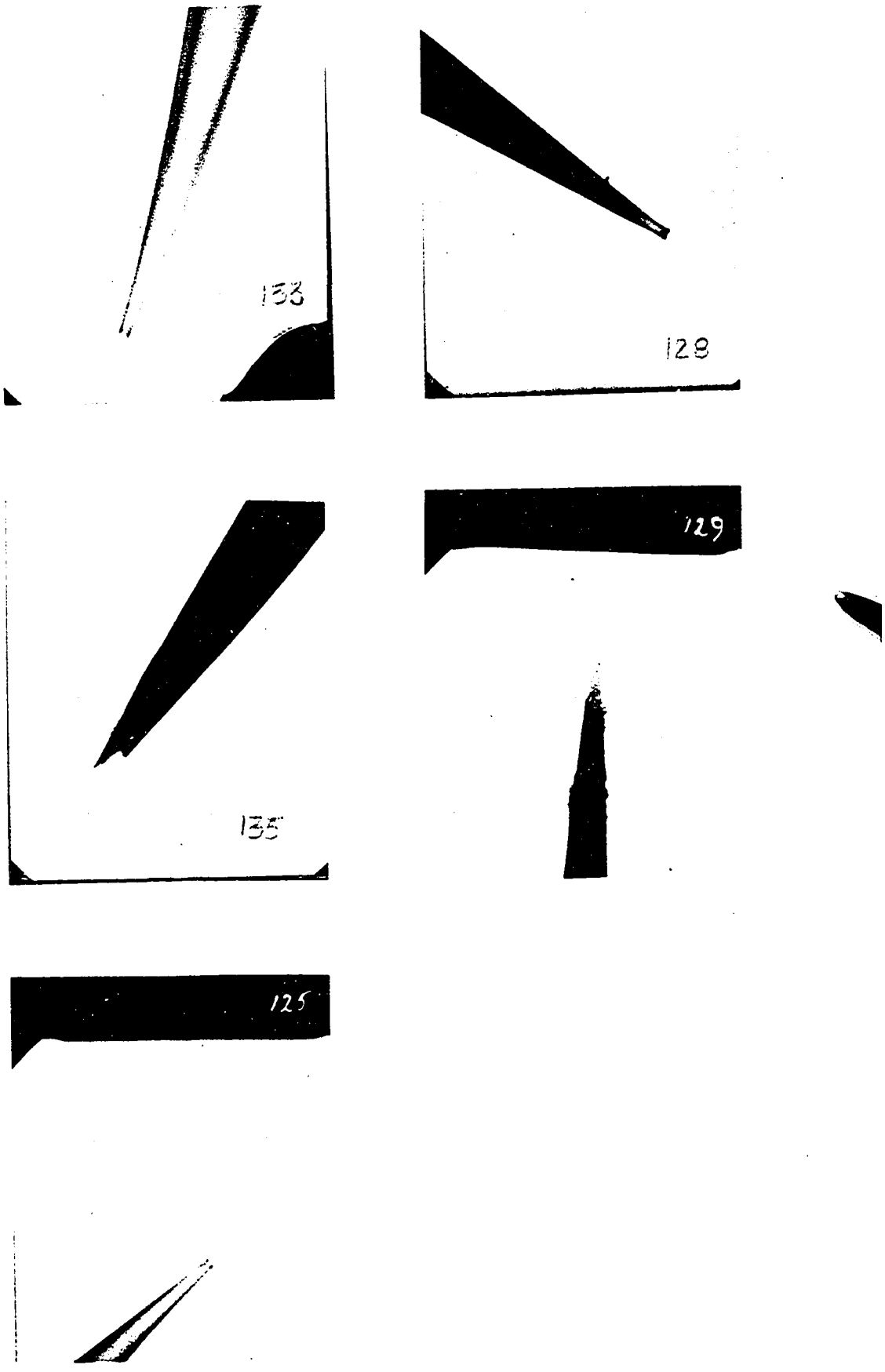

Fig. 5.8 Electron micrographs of microelectrodes (x7000)

(Courtesy of Dr. M. Colonnier, Department of Anatomy, University of Ottawa)

The microelectrodes filled with 3M KCl solution and having resistance less than 5 megohms have in general large tip diameter. Such electrodes are not suitable for membrane potential measurements because the ionic content of the cells can be altered by diffusion from the tip. When choosing electrodes of high resistance, uncertainties in the measurements may be introduced due to tip potential. This was pointed out by Adrian (24) on the basis of the following observations:

(1) Some electrodes with high resistance which penetrated the membrane of the muscle fibre without apparent damage gave very low resting potential in normal Ringer's solution. The mean of 19 impalements with an electrode of resistance 36 megohms was found to be 58.7 ± 0.6 mV. The mean value of the actual resting potential of these fibres was about 90 mV.

(2) Two electrodes might give very different mean values for the resting potential of the same muscle.

(3) Breaking an electrode which gave low values of the resting potentials if it was still usable, immediately increased the measured resting potential to about 90 mV.

That some kind of junction potential could account for these observations was concluded from the fact that although the recorded resting potential may be very low, the total size of action potential was not significantly altered. Large variations of the resting potential measurements can be introduced by the microelectrode and though this error seems to be directly related to the tip potential, electrodes of high resistance are more likely to give rise to this trouble than electrodes of low resistance.

The anomalous junction potential is assumed to be resulting from some kind of "blocking" at the tip and the mechanism is not clearly understood. However Adrian showed on the basis of experimental results that the uncertainty introduced by tip potential could be minimized by using electrodes with resistance greater than 5 megohms and negative tip potential between 0-5 mV.

APPENDIX I

DONNAN MEMBRANE EQUILLIBRIUM

Donnan deduced his theory for a system composed of two solutions separated by a membrane of a peculiar semi-i permeability. The membrane must be freely permeable to the solvent and to the most dissolved substances, including electrolytes, but absolutely impermeable to at least one species of ions present in the solution. This non-diffusible ion species is in one compartment only and is kept there by the impermeability of the membrane to it.

Suppose the electrolytes present to be HCl and ionized XCl, the membrane being impermeable to X^+ ions. The H^+ and Cl^- can penetrate the membrane and do so in pairs because of the electrostatic forces between them.

Fig.A1.1 shows distribution of these ions at equillibrium on the two sides of membrane

		Membrane	
a	X^+		
b	H^+	H^+	c
(a + b)	Cl^-	Cl^-	c

Then the Donnan equillibrium relation is expressed as

$$c^2 = b\,(a + b) \qquad \text{——————} \quad (1)$$

where a, b, c represent concentrations of

the ions shown. When no non-diffusible ion is present a = o and

$$c^2 = b^2$$ i.e., the diffusible ions would be equally distributed at equillibrium. For a time equillibrium as considered by Donnan the system will not do any work. If such a system is converted into a galvanic cell by the introduction of electrodes reversible with respect to one species of diffusible ions, the electromotive force (emf) of the cell will be zero. For example if AgCl-Ag wire is immersed into each compartment of the system containing XCl and HCl no emf should be found. This was found to be true experimentally.

As shown in equation 1, the concentration of H^+ or Cl^- in the two solutions are not equal, therefore it should result in unequal electrode potentials at the two AgCl-Ag electrodes. That this is not shown experimentally is because there is a third seat of potential difference; namely, between the two solutions on the opposite side of the membrane. Donnan predicted that such a membrane potential should exist and its value is given by a formula identical with Nernst formula for concentration cell

$$E_c = \frac{RT}{ZF} \ln \frac{C1}{C2}$$

where E_c is potential difference due to concentrations of ions C_1 and C_2 on the two sides of the membrane.

APPENDIX 2

MEMBRANE RESISTANCE AND CAPACITANCE

Considering the muscle fibre as a cable we can derive expressions for the resistance and capacitance of membrane.

Let us introduce the following designations:

d_i, the internal or core diameter of fibre (cm).

d_o, the outside diameter of fibre (cm).

t, thickness of membrane (cms).

m, specific resistance of membrane dielectric material (ohm . cm)

R_m, transverse membrane [illegible] unit length.

r_m, transverse resistance

= (resistance of m[illegible] length)

x (circumferenc[illegible]) (ohm. cm^2).

ε_m, relative dielectric constant of membrane.

C_m, membrane capacitance per unit length of fibre.

($\mu F/cm^2$)

(i) The transverse membrane resistance for a unit length of fibre, is the resistance between two concentric cylinders one unit in length separated by the thickness of membrane.

From Fig.A2.1 this resistance across a cylinder of infinitesimal thickness 'dx'

$$= \rho_m \frac{dx}{(2\pi x).1}$$

integrating between internal and external radii

$$R_m = \rho_m \int_{d_i/2}^{d_o/2} \frac{dx}{2\pi x} = \frac{\rho_m}{2\pi} \ln \frac{d_o}{d_i}$$

and by definition

$$r_m = (\pi d_o) \frac{\rho_m}{2\pi} \ln \frac{d_o}{d_i}$$

For thin membranes i.e., when difference between d_o and d_i is not large,

$$\ln \frac{d_o}{d_i} = \frac{d_o - d_i}{d_o} = \frac{2t}{d_o}$$

$$R_m = \frac{\rho_m t}{\pi d_o} \text{ cm and } r_m = \rho_m t \ \Omega.cm^2$$

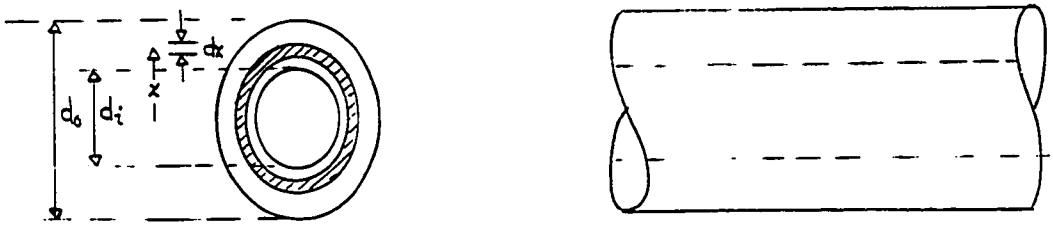

Fig. A2.1

(ii) From Fig.A2.1 if 'Q' is the charge stored in dielectric medium, S_x is the stress developed at 'x' and 'ε' denotes the absolute permittivity of the medium, then

$$\varepsilon S (2\pi x) = Q \qquad \text{(Gauss Theorem)}$$

and potential difference between the conductor and surface of sheath

$$E = \int_{d_i/2}^{d_o/2} S_x \, dx = \frac{Q}{2\pi\varepsilon} \ln \frac{d_o}{d_i}$$

$$= \frac{Q}{2\pi\varepsilon} \cdot \frac{2t}{d_o}$$

Capacitance per cm length

$$C = \frac{Q}{E} = \frac{\pi \varepsilon d_o}{t}$$

Hence membrane capacitance per unit area

$$C_m = \frac{C}{(\pi d_o)1} = \frac{\varepsilon}{t}$$

but $$\varepsilon = \varepsilon_m \cdot \varepsilon_o$$

where ε_o = permittivity of free space

= 8.855×10^{-8} μF/cm

$$\therefore \quad C_m = \frac{8.855 \times 10^{-8} E_m}{t} \quad \mu F/cm^2$$

APPENDIX 3

a. APPARATUS:

The length of fibres is an important factor in choosing the dimensions of the apparatus. We have been using fibres of about 1.5 cm length. In our apparatus, the middle chamber was about 1 cm long. The lengths of chambers 1 and 3 can be chosen arbitrarily and they were 0.8 cm long each in our case. All pieces were cut from plexiglass and cemented on a plexiglass base. The chambers were placed a small distance apart (1 mm). In order to isolate the adjacent chambers rectangular pieces of acetate paper were cemented on the surfaces facing each other in spaces S1 and S2. Suitable holes for the muscle fibres were pierced in the acetate paper. (Please see Fig.3.2)

b. ELECTRODES:

4 gms of agar was mixed with 100 cc of isotonic NaCl solution and the mixture was then heated. The resulting liquid was used to fill glass tubes corresponding to the diameter of holes E1 and E2. This liquid solidifies when cooled. Silver chloride (AgCl) was deposited electrolytically on silver wire (about 0.25 mm in dia.) in 120 mM NaCl solution, at a constant current of about .05 mA per electrode. These wires were then inserted in the filled glass tubes to make electrodes.

c. STOCK SOLUTIONS:

The following stock solutions were used to prepare (i) Ringer's solution and (ii) Depolarizing solution:

1M KCl solution

2M NaCl "

1M $CaCl_2$ "

10mM $CaSO_4$ "

380mM K_2SO_4 "

500mM $NaHCO_3$ "

d. COMPOSITION OF SOLUTIONS IN mM

(i) Ringer's solution

KCl	NaCl	$CaCl_2$	$NaHCO_3$
2.5	115	5	5

(ii) Depolarizing solution

KCl	$CaSO_4$	K_2SO_4	$NaHCO_3$
2.5	5	93.71	5

(iii) Sucrose solution

260 mM

This solution was prepared in 2X glass distilled water and passed through an ion exchanger to de-ionize.

APPENDIX 4

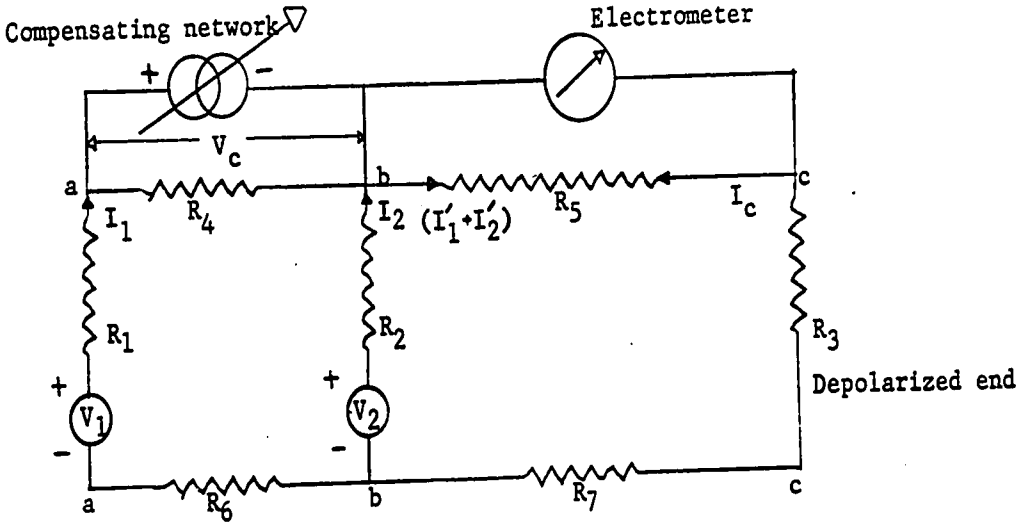

Fig. A4.1 The compensating network is connected across two chambers containing Ringer's solution as bathing fluid. The electrometer (null detector) is connected across chambers, one containing Ringer's solution and the other depolarizing solution. The chamber in between contains sucrose solution as bathing fluid.

Referring to the above figure

I_1 is the total current due to biological generator V_1

I_2 is the total current due to biological generator V_2

Applying Thevenin's Theorem

$$I_1 = \frac{V_1}{R_1 + R_4 + \left[R_2 /\!/ (R_5 + R_3 + R_7)\right] + R_6}$$

$$= \frac{V_1}{R_1 + R_2 + R_4 + R_6} \qquad \because\ R_5 \gg (R_3 + R_7) \text{ and } R_2 \ll R_5$$

Contribution from I_1 to R_5

$$= \frac{V_1}{R_1 + R_2 + R_4 + R_6} \times \frac{R_2}{R_5 + R_3 + R_7} = \frac{V_1}{R_1 + R_2 + R_4 + R_6} \times \frac{R_2}{R_5}$$

Similarly

$$I_2 = \frac{V_2}{R_2 + [(R_1 + R_4 + R_6) /\!/ (R_5 + R_3 + R_7)]}$$

$$= \frac{V_2}{R_1 + R_2 + R_4 + R_6}$$

Contribution from I_2 to R_5

$$= \left[V_2 - I_2 R_2\right] \times \frac{1}{R_5}$$

$$= V_2 \left[1 - \frac{R_2}{R_1 + R_2 + R_4 + R_6}\right] \frac{1}{R_5}$$

$$= V_2 \left[\frac{R_1 + R_4 + R_6}{R_1 + R_2 + R_4 + R_6}\right] \frac{1}{R_5}$$

If $V_1 = V_2$, then total contribution from I_1 and I_2 to R_5

$$I'_{(1+2)} = V \left[\frac{R_2}{R_1 + R_2 + R_4 + R_6} + \frac{R_1 + R_4 + R_6}{R_1 + R_2 + R_4 + R_6}\right] \frac{1}{R_5}$$

$$= \frac{V}{R_5}$$

To obtain null, let the compensating potential be V_c

Then the compensating current through R_5 as shown in Fig. A4.1

$$I_c = \frac{V_c}{R_1 + R_2 + R_6} \times \frac{R_2}{R_5} = \frac{V_c}{R_5} \times \frac{R_2}{R_1 + R_2 + R_6}$$

At null

$$I'_{(1+2)} = I_c$$

$$\frac{V_c}{R_5}\left[\frac{R_2}{R_1 + R_2 + R_6}\right] = \frac{V}{R_5}$$

$$V_c = \left[\frac{R_1 + R_2 + R_6}{R_2}\right] V$$

$$= \left[1 + \frac{R_1 + R_6}{R_2}\right] V$$

This shows that theoretically it is not possible to record the actual value of the resting potential by compensation method in the case of muscle fibres. The compensating potential would be about twice the actual resting potential. However the technique may still be useful in other measurements.

APPENDIX 5

The microelectrode is a glass capillary drawn into a fine tip about one micron in diameter and filled with some suitable electrolytic solution. The electrical connection from the micro electrode to the measuring instrument is made through a silver wire covered with silver chloride.

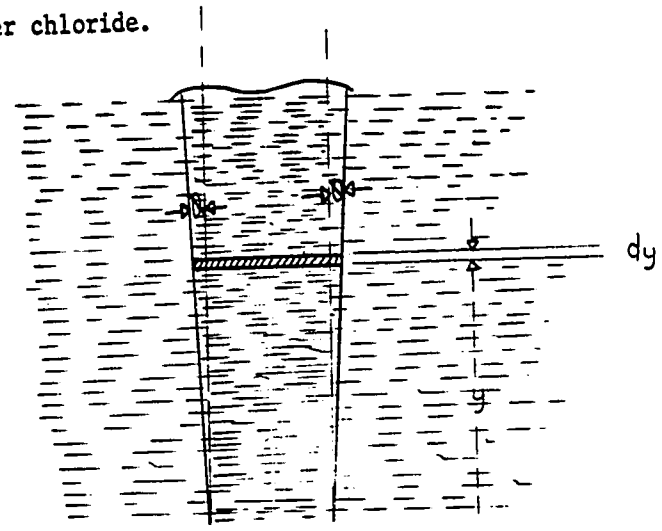

Fig.A5.1

The resistance of micro electrode consists of two components:

(i) R_{in}, resistance of the electrolyte inside micro-pipette

(ii) R_{ex}, resistance of the surrounding fluid between the tip of micro-electrode and other electrodes.

If in = sp. resistance of electrolyte inside electrode

Then, referring to Fig. 1

$$R_{in} = \rho_{in} \frac{\ell}{a}$$

$$= \rho_{in} \int_0^y \frac{dy}{\pi/4(D+2y \tan \phi)^2}$$

$$= \frac{4\rho_{in}}{\pi} \int_0^y (D+2y \tan \phi)^{-2} \, dy$$

$$R_{in} = \frac{4\rho_{in}}{\pi}\left[\frac{(d+2y\tan\phi)}{-2\tan\phi}\right]_0^y$$

$$= \frac{4\rho_{in}}{\pi}\left[\frac{1}{2d\tan\phi}\left(1+\frac{d}{2Y\tan\phi}\right)^{-1}\right]$$

Now $\frac{d}{2Y\tan\phi} \ll 1$

$$\therefore \quad R_{in} = \frac{2\rho_{in}}{\pi d\tan\phi} \qquad (1)$$

The external resistance R_{ex} is equivalent to the resistance two concentric spheres.

Surface area of the internal sphere

= tip area of micropipette

= $\pi d^2/4$

Therefore, radius of the internal sphere

= $d/4$

Let, radius of the external sphere be R

Then $R_{ex} = \rho_{ex} \cdot \ell/a$

$$= \rho_{ex}\int_r^R \frac{dx}{4\pi x^2}$$

$$= \frac{\rho_{ex}}{4}\left[4/d - \frac{1}{R}\right]$$

$$R_{ex} = \frac{\rho_{ex}}{d} - (2) \text{ because } 4/d \gg \frac{1}{R}$$

Hence total equivalent resistance of microelectrode

$$R_{eq} = \frac{1}{\pi d}\left[\frac{2\rho_{in}}{\tan\phi} + \rho_{ex}\right] - \qquad (3)$$

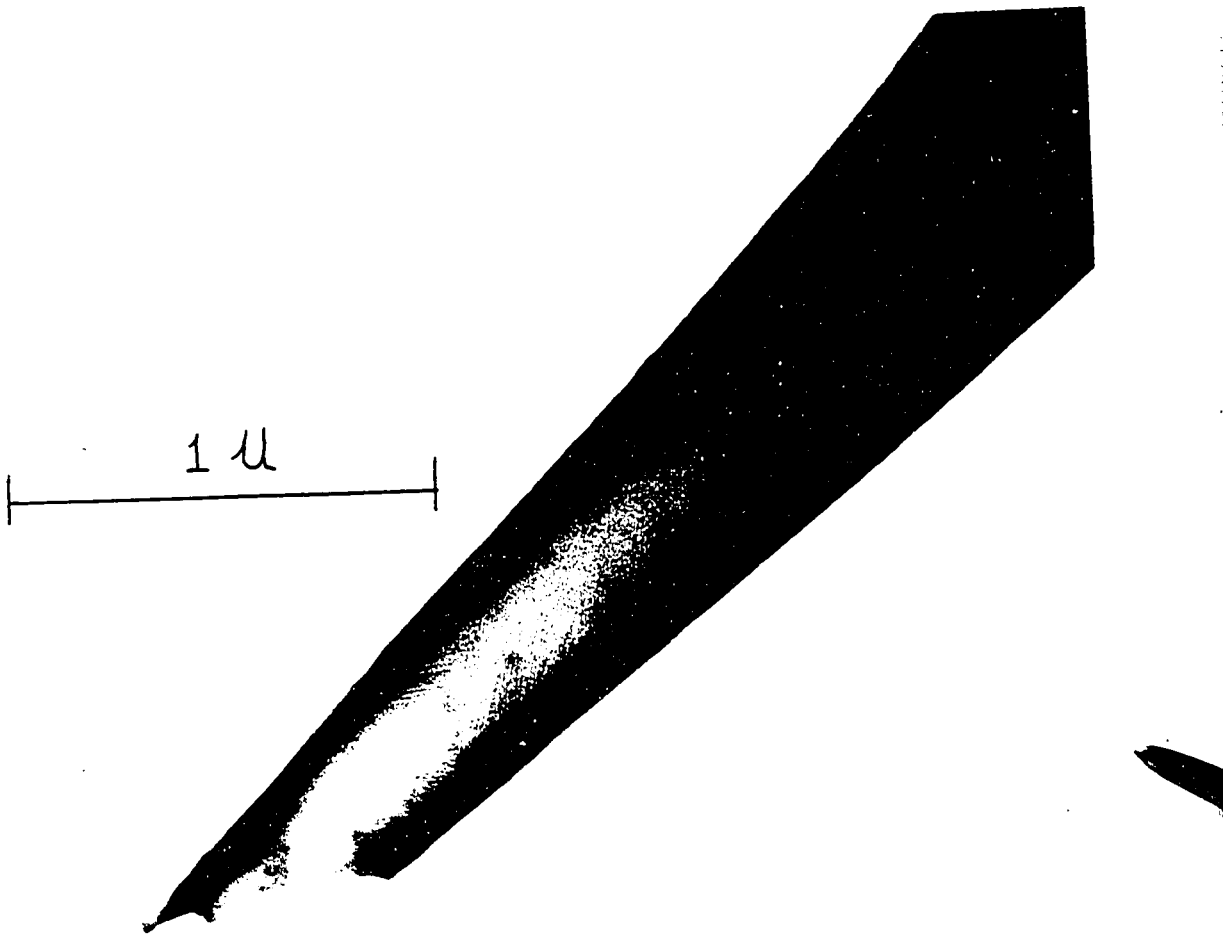

Figure A5.2

Electron micrograph of a typical microelectrode (x 66,000)

(Courtesy Dr. M. Colonnier, Anatomy Department, University of Ottawa)

Values of internal tip diameter and tan ϕ as estimated from Figure A5.2 are

$$d = 0.152\ \mu$$

$$\tan \phi = \frac{1}{30} \quad \text{(slope of internal surface)}$$

For use in the laboratory, the microelectrodes were filled with 3 molar KCl soln.

Sp. resistance of 3-molar KCl solution

$$\rho_{in} = 3.36\ \Omega\text{.cm}(**)$$

Specific resistance of the Ringer's solution used in the lab. was measured

$$\rho_{out} = 82\ \Omega\text{cm.}$$

Substituting these values in equation (3) of the appendix

$$R_{eq} = 5.94\ \text{M}\Omega$$

The average value of the measured resistance of microelectrodes was found to be about 10 MΩ .

The reason for the difference between calculated and measured resistance is not very obvious. It is possible that the specific resistance of KCl solution inside micropipette is higher than the value used for calculation.

(**) From J.F. Chambers, Jean M. Stokes and R.H. Stokes "Conductance of concentrated sodium and potassium chloride solutions at 25°" J. Phys. Chem. vol. 60 pp. 985 - 986, July 1956.

BIBLIOGRAPHY

1. Sanderson, J.B., "A report on Prof. L. Hermann's recent researches on the electromotive properties of muscle". (1928) J. Physiology, Vol. 1, pp. 196-212; (Reprint 1952).
2. Hermann, L., Pflugers Archiv., Vol. 38, p. 158.
3. Hermann, L., "The capillary electrometer and action current in muscle", Pflugers Archiv., Vol. 63, p.440: (1896).
4. Burch, G.J., "On a method of determining the value of rapid variations of a difference of potential by means of the capillary electrometer", Proc. Royal Soc., London, Vol. 48, pp. 89-93. (1890).
5. Sanderson, J.B., and G.J. Burch, "On the localization of the effect of injury in muscle", J. Physiol., Vol.15, pp. 17-18 (P).
6. Sanderson, J.B., "The electrical response to stimulation of muscle and its relation to mechanical response",
   Part I, J. Physiol., Vol. 18, pp. 117-157 (1895);
   Part II, J. Physiol., Vol. 18, pp. 325-358 (1895).
7. Forbes and Mache, (1920), Amer. Jour. Physiol., Vol.52, p. 409.
8. Gasser and Newcomer, (1921), Ibid. Vol. 57, p. 1.
9. Adrian, E.D., "The impulse produced by sensory nerve endings". Part I, J. Physiol., Vol. 61, pp. 49-72.
10. Cole, K.S., and H.J. Curtis, (1938) "Electric impedance of Nitella during activity". J. Gen. Physiology, Vol. 22, p. 37.
11. Young, J., (1936) "Structures of nerve fibres and synapses in some invertebrates", Cold Spring Harbour Symposia on Quantitative Biology, Vol. 4, p. 1.

12. Cole, K.S., and A.L. Hodgkin. (1939) "Membrane and protoplasmic resistance in the squid giant axon". J. Gen. Physiology, Vol. 22, p. 671.

13. Webb, D.A., and J. Young, (1940) "Electrolytic content and action potential of the giant nerve fibres of Loligo". J. Physiology, Vol. 98, p.299.

14. Steinback, H.B., (1940) "Chemical and concentration potentials in the giant fibres of squid nerves". J. Cell. and Comp. Physiol. Vol. 15, p. 373.

15. Hodgkin, A.L., and A.F. Huxley, (1939) "Action potentials recorded from inside a nerve fibre". Nature, Vol. 144, p. 710.

16. Curtis, H.J., and K.S. Cole, (1940) "Membrane action potentials from the squid giant axons". J. Cell. and Comp. Physiology, Vol. 15, p.147.

17. Graham, J., G.R. Carlson and R.W. Gerard, (1942) "Excitation and membrane potentials of single muscle fibres". Federation Proc., Vol. 1, p.31.

18. Gerard, R.W., and J. Graham, (1942) "Excitation and membrane potentials of single muscle fibres". Federation Proc., Vol. 1, p. 29.

19. Graham, J., and R.W. Gerard, (1946) "Membrane potentials and excitation of impaled single muscle fibres". J. Cell. and Comp. Physiology, Vol. 28, pp. 99-117.

20. Ling, G., and R.W. Gerard, "The normal membrane potential of frog sartorious fibres". (1949) J. Cell. and Comp. Physiol., Vol. 34, pp. 383-395.

21. Nastuk, W., and A.L. Hodgkin, (1950) "The electrical activity of single muscle fibres", J. Cell. and Comp. Physiol., Vol. 35, pp. 39-74.

22. Nastuk, W., "The electrical activity of the muscle cell membrane at the neuro-muscular membrane", J. Cell and Comp. Physiol., Vol. 42, pp. 249-272.

23. Del Castillo, J. and B. Katz, (1955) "Local activity at a depolarized nerve muscle juntion", J. Physiol., Vol. 128, pp. 396-411.

24. Adrien, R.H., (1956) "The effect of internal and external potassium concentration on the membrane potential of frog", J. Physiol., Vol. 133, pp. 631-658.

25. Mathews, Bryan, H.C., (1934) "A special purpose amplifier", J. Physiol., Vol. 81, pp. 28-29 (P)

26. Bernstein, (1912) Electrobiologie (Braunshweig)

27. Brunings (1903) Arch. f. d. ges Physiol., Vol. 98, p.241.

28. Lillie (1914) Amer. Journal of Physiology, Vol. 34, p. 414.
(1915) Amer. Journal of Physiology, Vol. 37, p. 348.
(1920) J. Physical Chem., Vol. 24, p.165.

29. Lillie (1920) J. Gen. Physiol., Vol. 3, p. 107.

30. Boyle, P.J., and E.J. Conway, (1941) "Potassium accumulation in muscle and associated changes", J. Physiol., Vol. 100, pp. 1-63.

31. Huxley, A.F., (1954) "Electrical processes in nerve conduction in ion transport across membranes", p. 23, New York Academic Press.

32. Hodgkin, A.L., "Ionic movements and electrical activity in giant nerve fibres", Proc. Royal Soc. London, Ser. B, Vol. 148, pp. 1-33, (1958).

33. Hodgkin, A.L., and A.F. Huxley, "A quantitative description of membrane current and its application to conduction and excitation in giant axon of nerve", J. Physiol. (1952) Vol. 117, pp. 500-544.

34. Goldman, D.E., "Potential, Impedance and Rectification in Membranes", J. Gen. Physiol. (1943), Vol. 27, pp. 37-60.

35. Hodgkin, A.L., and B. Katz, (1949 a) "The effect of Na^{+} ions on the electrical activity of giant axon of squid", Arch. Sci. Physiol., Vol. 3, p.129.

36. Hodgkin, A.L., "The ionic basis of electrical activity in nerve and muscle", Biol. Review, Cambridge Physiol. Soc. (1951) Vol. 26, pp. 339-401.

37. Adrian, R.H., and W.H. Freygang, "The potassium and chloride conductance of frog muscle membrane", J. Physiol. (1962) Vol. 163, No. 1, pp. 61-103.

38. Parapart, A.K., and R. Ballantine, (1952); in Modern Trends in Physiology and Biochemistry, (Barron, E-S-G., ed.) Academic Press, New York, p.135.

39. Clark, F.M., "The properties of dielectrics: part II, the dielectric constants", J. Franklin Institute, Vol. 208, July - Dec., 1929, pp. 17-44.

40. Davson, H., and J.F. Danielli, (1952) "Permeability of natural membranes", 2nd Ed., Cambridge University Press, London.

41. Schmitt, F.O., and K.J. Palmer, "X-ray diffraction studies of lipids and lipide-protein systems", Cold Spring Harbour Symposia Quant. Biol., 8, 94, 1940.

42. Ruch, T.C., and J.F. Fulton,"Medical Physiology and Biophysics", (1960), W.B. Saunders Company, Philadelphia and London, pp. 48 and 14.

43. Katz, B., "The electrical properties of muscle fibre membrane", Proc. Royal Soc., London, Dec. 1948, pp. 506-534.

44. Huxley, A.F., and R. Stampfli, "Direct determination of membrane resting potential and action potential in simple myelinated nerve fibres", J. Physiol., Vol. 112, pp. 476-495, (1951).

45. Stampfli, R., "A new method for measuring membrane potentials with external electrodes", Experimentia, Vol. 10, pp. 508-509, (1954).

46. Grundfest, H., "Instrument Requirements and Specifications in Bioelectric Recording", Ann. N.Y. Acad. SCI., Vol. 60, pp. 841-859.

47. Bell, P.R., "Negative Capacity Amplifier, M.I.T. Rad. Lab. Ser., McGraw-Hill Book Co. Inc., N.Y. Vol. 19, app.A, 1949.

48. Woodbury, J.W., "Recording Central Nervous Activity with Intr-cellular Ultramicroelectrodes: Use of Negative Capacity Amplifier to Improve Transient Response", Fed. Proc. Vol. 12, p. 159, March '53.

49. Solms, S.J., W.L. Nastuk and J.T. Alexander, "Development of a High-fidelity Preamplifier for Use in Recording of Bioelectric Potentials with Intracellular Electrodes", Rev. Sci. Inst. Vol. 24, p. 960-967, October, 1953.

50. Happanon, L., and D. Ottoson, "A High Frequency Compensated Input Unit for Recording with Microelectrodes", Acta. Physiol. Scand. Vol. 32, p. 271-280, 1954.

51. Amatniek, E., "Measurements of Bioelectric Potentials with Microelectrodes and Neutralized Input Capacity Amplifiers", IRE Trans. on Medical Electronics, Vol. PGME-10, pp. 3-14, March 1958.

52. Guld, Christian, "Cathode Follower and Negative Capacitance as High Input Impedance Circuits", Proc. IRE, Vol. 50, No. 9 pp. 1912-1927, September, 1962.

53. van der Ziel, A., "Noise", Prentice-Hall Electrical Engineering Series, N.Y., Chapter 2.

54. Savaetichin, G. (1951) "Low resistance microelectrodes", Acta Physiol. Scand., Vol. 24, Suppl. 86, pp. 5-13.

55. Gestleland, R.C., B. Howard, J.Y. Lettvin and W.H. Pitts, "Comments on microelectrodes", Proc. IRE, Nov. 1959, pp. 1856-1862.

56. Nastuk, W.L., and A.L. Hodgkin (1950) "The electrical activity of single muscle fibres", J. Cell and Comp. Physiol., Vol. 35, 1950, p. 39.

57. Winsbury, G.J., (1956) "Machine for the production of micro-electrodes", Rev-Sci. Inst., Vol. 27, No. 7, pp. 514-516.

VITA

NAME: Syed Imtiaz Ahmad

BORN: Lucknow, India, Dec. 1, 1941.

EDUCATED:

Primary: Muslim High School, Rawalpindi, Pakistan.

Secondary: Gordon College, Rawalpindi, Pakistan.

University: Government College of Engineering and Technology, University of Panjab, Lahore, Pakistan.

Course: Electrical Engineering (Power and Communication).

Degree: B.Sc. (Engineering).